

A Versatile Tripodal Cu(I) Reagent for C–N Bond Construction via Nitrene-Transfer Chemistry: Catalytic Perspectives and Mechanistic Insights on C–H Aminations/Amidinations and Olefin Aziridinations

Vivek Bagchi,[†] Patrina Paraskevopoulou,[‡] Purak Das,[†] Lingyu Chi,[†] Qiuwen Wang,[†] Amitava Choudhury,[†] Jennifer S. Mathieson,[§] Leroy Cronin,^{*,§} Daniel B. Pardue,^{||} Thomas R. Cundari,^{*,||} George Mitrikas,[⊥] Yiannis Sanakis,[⊥] and Pericles Stavropoulos^{*,†}

[†]Department of Chemistry, Missouri University of Science and Technology, Rolla, Missouri 65409, United States

[‡]Inorganic Chemistry Laboratory, Department of Chemistry, University of Athens, Panepistimiopolis Zografou 15771, Athens, Greece

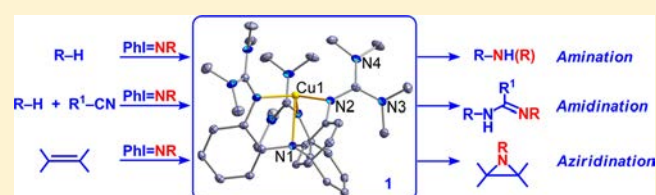
[§]School of Chemistry, University of Glasgow, University Avenue, Glasgow, G12 8QQ, U.K.

^{||}Department of Chemistry, Center for Advanced Scientific Computing and Modeling (CASCaM), Denton, Texas 76203, United States

[⊥]Institute of Advanced Materials, Physicochemical Processes, Nanotechnology and Microsystems, NCSR “Demokritos”, Ag. Paraskevi 15310, Athens, Greece

S Supporting Information

ABSTRACT: A Cu^I catalyst (**1**), supported by a framework of strongly basic guanidinato moieties, mediates nitrene-transfer from PhI=NR sources to a wide variety of aliphatic hydrocarbons (C–H amination or amidination in the presence of nitriles) and olefins (aziridination). Product profiles are consistent with a stepwise rather than concerted C–N bond formation. Mechanistic investigations with the aid of Hammett plots, kinetic isotope effects, labeled stereochemical probes, and radical traps and clocks allow us to conclude that carboradical intermediates play a major role and are generated by hydrogen-atom abstraction from substrate C–H bonds or initial nitrene-addition to one of the olefinic carbons. Subsequent processes include solvent-caged radical recombination to afford the major amination and aziridination products but also one-electron oxidation of diffusively free carboradicals to generate amidination products due to carbocation participation. Analyses of metal- and ligand-centered events by variable temperature electrospray mass spectrometry, cyclic voltammetry, and electron paramagnetic resonance spectroscopy, coupled with computational studies, indicate that an active, but still elusive, copper-nitrene (*S* = 1) intermediate initially abstracts a hydrogen atom from, or adds nitrene to, C–H and C=C bonds, respectively, followed by a spin flip and radical rebound to afford intra- and intermolecular C–N containing products.



I. INTRODUCTION

Atom/group transfer chemistry¹ mediated by transition-metal reagents is a powerful methodology for the engagement of transferrable atoms (hydrogen,² nitrogen,³ oxygen,⁴ sulfur,⁵ halogen⁶) or groups (boryl,⁷ carbene,⁸ nitrene⁹) in the activation of C–H and C=C bonds to construct new C–X functionalities. Among different C–N bond installation approaches,¹⁰ metal-catalyzed nitrene insertions into C–H/C=C bonds to afford amination/aziridination products⁹ reign supreme in the synthetic chemist’s arsenal and have even provided examples of biological significance.¹¹ Although many metal reagents (especially of the coinage metals¹² and Rh,¹³ but also of Fe,¹⁴ Co/Ir,¹⁵ Ni,¹⁶ and Mn/Ru¹⁷) have been devised to facilitate nitrene-transfer chemistry, significant challenges remain in assembling atom-economical and environmentally friendly catalytic processes that enjoy high turnover numbers and selectivity. In particular, C–H amination reactions have

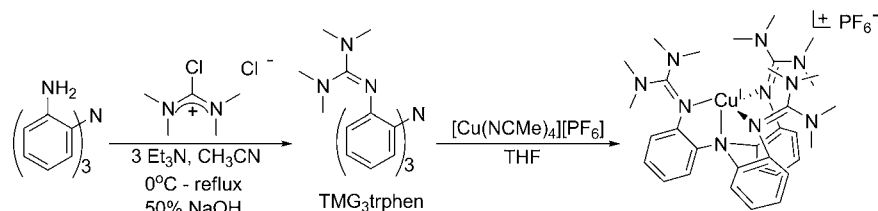
only recently evidenced the development of practical reagents that supersede the historical porphyrinoid paradigms¹⁸ and make use of Earth-abundant first-row transition elements. Moreover, mechanistic arguments,¹⁹ even for the better established olefin aziridination reactions,²⁰ are far from settled, especially in relation to (i) the mode of nitrene transfer from suitable precursors (usually ArI=NR, RN₃, RNNaX) to the metal moiety, (ii) the electronic description of the catalytically active, albeit elusive, metal nitrene species (M=NR),^{12a,21} and (iii) the manner by which the insertion/addition of nitrene to the acceptor substrate takes place (concerted, stepwise).

In this report, a novel tripodal Cu^I reagent is presented that is capable of mediating a wide range of alkane amination and alkene aziridination reactions, as well as a rarely observed three-

Received: April 17, 2014

Published: July 15, 2014

Scheme 1



component addition to nitriles to provide amidinates. Furthermore, the present catalyst enables the mechanistic distinction of the two components of the stepwise nitrenoid insertion operation, i.e., hydrogen abstraction/C–N recombination in aminations and nitrene addition/ring closure in aziridinations. Moreover, this work highlights the importance of carboradicals and carbocations in determining the product profile and pinpoints complexities arising from solvent-cage effects. Finally, while the majority of copper aziridination reagents (including seminal chiral examples²²) feature C_2 -symmetric ligands,²³ the current work investigates a catalyst with the less explored C_3 -symmetric coordination geometry,^{12e–g,o,p} supported by a highly basic, guanidinate-rich framework that has recently found wide use in metal–oxo and metal–dioxygen chemistry.²⁴

II. RESULTS AND DISCUSSION

1. Synthesis and Catalysis. a. Synthesis and Characterization of the Cu(I) Reagent. The tris[(tetramethylguanidino)phenyl]amine ligand (TMG₃trphen) used is readily prepared from the previously reported 2,2',2''-triaminotriphenylamine²⁵ and the preformed chlorotetramethylformamidinium chloride (Scheme 1). Metalation by $[\text{Cu}^{\text{I}}(\text{CH}_3\text{CN})_4][\text{PF}_6]$ in THF, followed by recrystallization from DMF, affords $[\text{Cu}^{\text{I}}(\text{TMG}_3\text{trphen})][\text{PF}_6]$ (**1**).

Compound **1** possessed a rigorous C_3 -symmetric coordination environment in the solid state, which features four distinct sets of methyl groups on the TMG arms, one of them [C(10)] pointing endo with respect to the metalated cavity [Figure 1

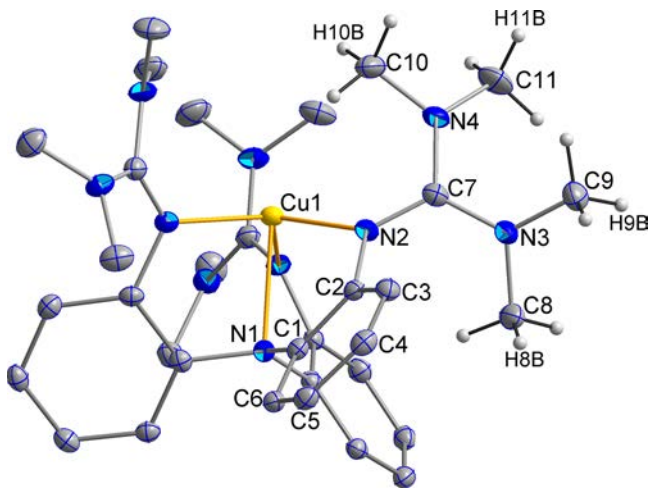


Figure 1. ORTEP diagram of **1** (cation only), drawn with 40% thermal ellipsoids. Selective interatomic distances (Å) and angles (deg): Cu(1)–N(1) = 2.355(2), Cu(1)–N(2) = 2.0129(15), N(2)–C(7) = 1.320(2), N(3)–C(7) = 1.366(2), N(4)–C(7) = 1.360(2); N(1)–Cu(1)–N(2) = 78.54(4), N(2)–Cu(1)–N(2A) = 116.15(3).

and Table S1, Supporting Information (SI)]. ¹H NMR data in CD₃CN solutions show that all four methyl groups [C(8)–C(11)] coalesce to a broad signal (2.587 ppm) at 70 °C, indicating simultaneous exchange due to rotation around all three N(2,3,4)–C(7) bonds. It is worthwhile noting that the N(2)–C(7) bond [1.320(2) Å] is elongated vs typical C=N bonds in guanidines²⁶ and the corresponding bond in $[\text{Cu}^{\text{I}}(\text{TMG}_3\text{tren})]\text{Cl}$,²⁷ presumably due to metalation and proximity to the aromatic group. The rotation is progressively restricted with decreasing temperature (Figures S3 and S4, SI), and eventually all four methyl groups resolve to four distinct peaks [δ (ppm, CD₃CN, –30 °C) = 3.078 (H(10)), 2.743 (H(11/9)), 2.683 (H(9/11)), 1.489 (H(8))].²⁸ Peak assignments were assisted by theoretical calculations [B3LYP/6-311+G(2,d,p) single point NMR property determination at the B3LYP/6-31G(d)-optimized geometry of **1**]. The highest field peak is most likely due to the H(8) protons, which reside in the shielded region of the aromatic groups. The lowest-field peak is best accommodated by the H(10) protons, pointing inward with respect to the vacant cavity. The outward oriented protons H(9) and H(11) are most likely responsible for the closely spaced peaks in the intermediate field, with the first assignment noted in the brackets above providing the best computational fit. The mononuclear structure is retained in solution according to ESI-MS data ($m/z = 647.35$, $[\text{Cu}^{\text{I}}(\text{TMG}_3\text{trphen})]^+$).

b. Catalytic Aminations. Amination with catalyst **1** of a wide variety of C–H-containing substrates has proven to be most productive with an excess of PhI=NTs (2 equiv) over substrate and 10 mol % catalyst in a variety of solvents [acetonitrile, acetonitrile/chlorobenzene (1:10 v/v), nitromethane] at room temperature (12 h reaction). Table 1 summarizes representative examples. Amination products for which crystallographic data are available are noted in Table S2 (SI).

The most challenging cycloalkanes (entries 1–3) undergo aminations in nitromethane, featuring yields that are competitive to those reported with Rh^{13a,d} and coinage-metal reagents, frequently employing excess substrate (≥ 5 equiv over nitrene).^{12e,f,i} Tertiary C–H positions (entries 4 and 5, Table 1) are regioselectively aminated in good yields, especially for the sterically encumbered tertiary C–H bonds of adamantane. Yields for the *tert*-C–H sites are comparable to those reported for Rh,^{13a,d} Mn/Ru,^{17b–e} and Ag^{12f} nitrene-transfer catalysts.

Benzylic substrates (entries 6–14, Table 1) can readily undergo nitrene insertion in various solvents, with the best yields obtained largely in acetonitrile. As anticipated, primary benzylic positions (entry 6; for toluene derivatives see below) are most challenging to aminate. The yields obtained are analogous to those reported with other Cu reagents^{12b,d,e} and superior to those associated with Rh^{13d} and Co^{15g} nitrene-transfer chemistry. Secondary benzylic positions (entries 7–10) are readily and regioselectively aminated, with yields crudely increasing with decreasing C–H bond-strength values.

Table 1. Amination (NHTs) of Hydrocarbons by **1**^a

Entry No.	Substrate	Products	Yield (%)
1.			49 ^b
2.			49 ^b
3.			66 ^b
4.			72 ^c
5.			36 ^c
6.			47 ^d
7.			53, 4, 4 ^b
8.			87 ^d
9.			42, 10 ^d
10.			92 ^d
11.			74 ^d 10 ^d
12.			66, 4 ^d
13.			68 ^d
14.			13, 79 ^d
15.			81 ^d
16.			45 ^d

^aReaction conditions: **1**, 0.025 mmol; substrate, 0.25 mmol; PhI=NTs, 0.50 mmol; solvent, 0.15 mL; molecular sieves (5 Å), 20 mg; *t* = 12 h. ^bIn nitromethane. ^cIn acetonitrile/chlorobenzene (1:10 v/v). ^dIn acetonitrile.

Specifically for ethylbenzene (entry 7), tetralin (entry 9), cumene (entry 12), and 9,10-dihydroanthracene (entry 14), products of desaturation (olefination/aziridination, aromatization) are also observed, along with traces of the precursor olefins. These products may arise from leakage of benzylic carbocations and subsequent E1-type proton elimination,²⁹ or via double H atom abstraction by metal-centered moieties³⁰ (see below for more details). In addition, the amination product of 9,10-dihydroanthracene decomposes slowly to anthracene and TsNH₂ (approximately 60% deamination over 12 h). Yields for ethylbenzene (entry 7) are somewhat lower than those obtained by Rh^{13a,d} and Cu^{12d} catalysts. On the other hand, the present copper reagent is, on average, more efficient than Rh¹³ and Cu¹² catalysts, as well as porphyrinoid Mn/Ru^{17c-e} and Co^{15a-d} reagents, for the amination of sterically encumbered *sec*-benzylic substrates. The same

attribute is noticeable with *tert*-benzylic sites (entries 11–13), with yields frequently exceeding reported values, especially for the sterically sensitive rhodium catalysts.^{13a,d} Heteroatoms readily direct NTs insertions into the vulnerable α-C–H positions (entries 15 and 16). The initial product of diphenylmethanamine amination is highly sensitive to TsNCH₂– loss upon workup, leading to substrate demethylation.³¹ Finally, it is noteworthy that no aromatic functionalization is observed, which can frequently betray the intervention of diffusively free nitrene radicals, in sharp contrast to the Tp³M (M = Cu, Ag)-catalyzed aromatic aminations.^{12e,f}

c. Catalytic Amidinations. In pure MeCN, a limited number of substrates, largely those featuring *tert*-C–H sites, afford products of MeCN insertion (amidines), with concomitant suppression of the yields of the usual amination products. Tables 2 and S3 (SI) illustrate the products of amidination for

Table 2. Amidination of Substrate *tert*-C–H Bonds by **1**^a

Entry No.	Substrate	Products	Yield (%)
1.			30, 31 ^b
2.			20, 38 ^c
3.			27 ^b
4.			32 ^c
5.			20, 6, 3, 3 ^b
6.			16, 8, 4, 4 ^c

^aReaction conditions: **1**, 0.025 mmol; substrate, 0.25 mmol; PhI=NTs, 0.50 mmol; solvent, 0.15 mL; molecular sieves (5 Å), 20 mg; *t* = 12 h. ^bIn acetonitrile. ^cIn benzonitrile.

tert-C–H bonds, with the assistance of three representative substrates and two nitriles (MeCN, PhCN) employed as solvent. In one instance, insertion of MeCN in the amination of ethylbenzene was observed in minute yields (Figure S10, SI).

The amidination products in entries 1–3 (Tables 2 and S3, SI) have been crystallographically characterized. For the mechanistically diagnostic substrate *cis*-1,4-Me₂-cyclohexane (entries 3 and 4), only one product of RCN insertion is obtained, indicating loss of stereochemical integrity (Figure 2). The diequatorial configuration (*trans*) of the two methyl groups, along with the axial positioning of the amidine moiety in the MeCN-inserted product, is also established by computational work as the lowest-energy conformation (Figure S5, SI). The same conformation is deduced from NMR analysis (Figures S6–S9, SI) for the PhCN-inserted product (Table 2, entry 4). At least three amination products can also be observed in conjunction with the amidination product of *cis*-1,4-Me₂-cyclohexane in both MeCN and PhCN, but so far we have not

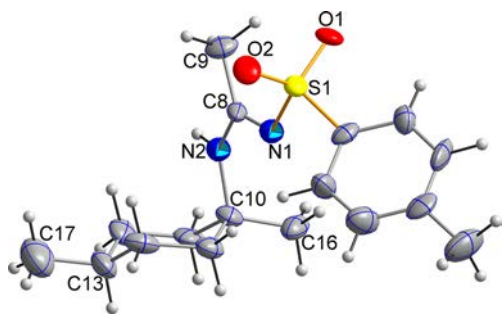


Figure 2. ORTEP diagram of the product obtained from the amidination of *cis*-1,4-Me₂-cyclohexane in MeCN (Table 2, entry 3), drawn with 40% thermal ellipsoids. Selective interatomic distances (Å) and angles (deg): N(1)–C(8) = 1.309(8), N(2)–C(8) = 1.340(8), N(2)–C(10) = 1.493(8), C(8)–C(9) = 1.498(8); N(1)–C(8)–N(2) = 118.8(5), N(2)–C(8)–C(9) = 114.7(6).

been able to separate and unambiguously characterize these products.³² The case of 2-methylbutane (entries 5 and 6) is particularly informative, because in addition to the expected amidination product, two isomeric aziridines were obtained in low yields, presumably via aziridination of the precursor olefins,^{12p} while the amidination product is notably present in suppressed amounts.

Acetonitrile-insertion byproducts have been mentioned in passing by Evans in allylic amidinations (NTs) of cyclohexene mediated by M(TPP)⁺ and M(OTf)₂ reagents (M = Mn, Fe; TPP = tetraphenylporphyrin).^{12q} They have been attributed to nonradical [2 + 2] addition of the M=NTs and N≡CR moieties, followed by rearrangement to generate the nitrenoid M=N–C(=NTs)R. However, the present Cu^I-residing cavity is unlikely to accommodate a [2 + 2] rearrangement, and there is no indication that activation of nitriles takes place by the 1/PhI=NTs system in the absence of any other substrate. Furthermore, the presumed nitrenoid would have been expected to conduct amidinations, and potentially aziridinations, on a more extensive list of substrates.

A more straightforward explanation to account for the nitrile-inserted products shown in Table 2 is provided by the Ritter-type addition of carbocations to the nitriles via the N atom terminus (R⁺ + R'C≡N → R'C⁺=N–R, further illustrated in Scheme 6 below).³³ This mechanistically diagnostic reaction distinguishes between carboradicals and carbocations,³⁴ since the former largely add to the carbon atom of the nitrile to generate iminyl radicals [R• + R'C≡N → (R')(R)C=N•] among other reactions.³⁵ The interference of carbocations is also evident in the formation of the olefin precursors of the aziridination products (entries 5 and 6), as expected for carbocations participating in E1-type proton eliminations. Further elaboration on the involvement of carbocations in predominantly carboradical-based chemistry is provided in the concluding section.

d. Catalytic Aziridinations. Aziridination of a panel of olefins (2.0 mmol) by the imidoiodinane PhI=NTs (0.25 mmol) was conducted in various solvents (MeCN, chlorobenzene, DMF, CH₂Cl₂) in the presence of catalytic amounts of **1** (0.0125 mmol). Reactions in MeCN (0.15 mL) usually afford the highest yields, and those are collected in Tables 3 and S4 (SI). Entries 1–9 feature a series of electron-diverse, para- and/or ortho-substituted styrenes, which undergo facile aziridination with excellent yields and speed (some reactions are complete in less than 30 min). More moderate results are

Table 3. Aziridination (NTs) of Olefins by **1**^a

Entry No.	Substrate	Products	Yield (%)
1.		R = H	>99
2.		R = Me	99
3.	R-	R-	R = ^t Bu >99
4.		R = OMe >99	
5.		R = F >99	
6.		R = Cl >99	
7.		R = CF ₃ 99	
8.		R = NO ₂ >99	
9.			78
10.			64
11.			92
12.			74
13.			94 c/t 41/59
14.			X = H >99 X = Ts c/t 27/73
15.			66
16.			55, 27
17.			n = 1 58, 12
18.			n = 2 69, 7
19.			n = 4 95
20.			42
21.			95, 3
22.			R = Me 84
23.			R = ^t Bu 95
24.			70
25.			74
26.			82 c/t 78/22
27.			86 c/t 78/22

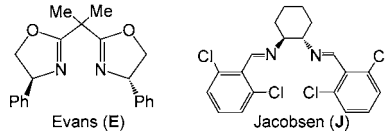
^aReaction conditions: **1**, 0.0125 mmol; substrate, 2.0 mmol; PhI=NTs, 0.25 mmol; acetonitrile, 0.15 mL; molecular sieves (5 Å), 20 mg; *t* = 2 h.

observed only in the aziridination of the bulky, ortho-substituted 2,4,6-trimethylstyrene (entry 9). Equally good yields, albeit at slower speeds, are observed in the aziridination of α -substituted styrenes (entries 10 and 11), with the caveat that the olefin amidination product is isolated for α -Ph, due to

facile ring-opening under the reaction and/or workup conditions (confirmed with the authentic aziridine). Two mechanistically instructive β -substituted (Me, Ph) styrenes afforded excellent yields in their *cis* configuration (entries 13 and 14), but with scrambling of stereochemistry, accentuated by bulk. The corresponding *trans* β -substituted styrenes (entries 12 and 15) provide *trans*-aziridines in more moderate yields. Entry 16 provides an example in which both aziridination and benzylic amination occur, albeit the former dominates the product profile. A series of cycloalkenes (entries 17–19) provide good to excellent conversions to the corresponding aziridines, the yield improving with increasing electron-rich character, but also decreasing due to the concomitant generation of allylic amination products. *exo*-Enes such as methylenecyclohexane (entry 21) are very efficiently aziridinated, as are electron-deficient alkyl acrylates (entries 22 and 23) and electron-rich, alkyl-substituted olefins (entries 24–27). The aziridinations of the electron-rich *cis*-alkenes (entries 26 and 27) provide significantly better retention of stereochemistry than that obtained for *cis*- β -methylstyrene (entry 13), but the *cis/trans* selectivities do not necessarily indicate any mechanistic shift toward concerted addition of the nitrene moiety for the alkyl-substituted olefins (see below).

For comparative purposes, the stereospecificity of the aziridination (PhI=NTs, 0.25 mmol) of *cis*-2-hexene (2.0 mmol) was examined with the aid of several common copper sources (0.0125 mmol) and two iconic chiral auxiliary ligands (0.0137 mmol), Evans' 2,2'-isopropylidenebis[(4*S*)-4-phenyl-2-oxazoline] (E)^{22b,36} and Jacobsen's (1*R*,2*R*)-bis((2,6-dichlorobenzylidene)diamino)cyclohexane (J),^{22a} in MeCN or CH₂Cl₂. Isomer ratios (*cis/trans*) are collected in Table 4. The

Table 4. Aziridination (NTs) of *cis*-2-Hexene by Cu/Ag Reagents^a



entry	Cu/Ag reagent	ligand	solvent	aziridine (<i>cis/trans</i>)
1	Cu(OTf) ₂ ·toluene	E	MeCN	67/33
2	Cu(OTf) ₂ ·toluene	E	CH ₂ Cl ₂	62/38
3	[Cu(NCMe) ₄] ₂ PF ₆	E	MeCN	72/28
4	[Cu(NCMe) ₄] ₂ PF ₆	E	CH ₂ Cl ₂	74/26
5	Cu(OTf) ₂	E	MeCN	69/31
6	[Cu(NCMe) ₄] ₂ PF ₆	J	MeCN	94/6
7	[Cu(NCMe) ₄] ₂ PF ₆	J	CH ₂ Cl ₂	95/5
8	[Cu(NCMe) ₄] ₂ PF ₆		MeCN	92/8
9	[Ag ^I (TMG ₃ trphen)]PF ₆		MeCN	no products

^aReaction conditions: **1**, 0.0125 mmol; ligand, 0.0137 mmol; substrate, 2.0 mmol; PhI=NTs, 0.25 mmol; solvent, 0.15 mL; molecular sieves (5 Å), 20 mg; *t* = 2 h; room temperature.

Evans auxiliary seems to be associated with significant loss of stereochemistry (entries 1–5), the best result (entry 4) being essentially equivalent to that observed with the system **1**/PhI=NTs (entry 26, Table 3). In contrast, Jacobsen's ligand furnishes superior stereocontrol (entries 6 and 7). In the absence of any specific ligand, [Cu(NCMe)₄]₂PF₆ alone provided high stereospecificity (entry 8), in agreement with

similar results previously reported.^{12q} The ligandless system has reportedly provided significant loss of stereocontrol in the aziridination of styrenes; hence, a dichotomy has been proposed^{12q} and since propagated in the literature²⁰ between alkyl-substituted olefins that undergo concerted aziridinations and styrenes that are candidates for stepwise nitrene-transfer. However, the results of Table 4 with *cis*-2-hexene suggest that scrambling of stereochemistry is experienced in all cases examined, albeit to a variable degree. The Ag^I congener³⁷ of **1** (entry 9) does not provide any products of aziridination, in contrast to Pérez's Cu^I and Ag^I C₃-symmetric reagents, which are both active catalysts.^{12e,f} Finally, it has been reported that the corresponding [Cu^I(TMG₃tren)]⁺ does not react when mixed with PhI=NTs.³⁸

Notably, the system **1**/PhI=O/TsNH₂ is equally effective in aziridinations, but **1**/PhI(O₂C^tBu)₂/TsNH₂ is unproductive, due to ligand stripping and formation of [Cu₂(O₂C^tBu)₄].

2. Mechanistic Studies. *a. Hammett Plots. i. Aziridinations.* Competitive aziridination reactions of a panel of para-substituted styrenes (1.0 mmol) vs styrene (1.0 mmol) by PhI=NTs (0.25 mmol) or PhI=NNs (Ns = -SO₂C₆H₄-*p*-NO₂) in the presence of **1** (0.0125 mmol) in MeCN have permitted the construction of Hammett plots (Figure 3, top, and Tables S5 and S6, SI) with the assistance of ¹H NMR spectroscopy. Most intriguing, and counterintuitive for an electrophilic reaction, is the observation that styrenes with electron-withdrawing substituents are more reactive than styrene itself in aziridinations by NTs (with the exception of CF₃), albeit not by NNs (with the exception of Cl). Pérez and Templeton have previously noted^{12g} the "slightly accelerating" effect of electron-withdrawing substituents in the aziridination (NTs) of para-substituted styrenes by Cu^I hydrotrispyrazolyl borate catalysts, and several copper-mediated aziridinations (NTs) by Evans^{12q} point to the same effect. As a consequence, for NTs aziridinations, typical polar substituent constant parameters (σ_p , σ^+ , σ_{mb}) provide poor correlations. In contrast, application of Jiang's dual-parameter correlation for radical reactions [$\log(k_X/k_H) = \rho_{mb}\sigma_{mb} + \rho_{JJ}\sigma_{JJ} + C$],³⁹ which combines both polar substituent (σ_{mb}) and spin-delocalization constant (σ_{JJ}^*) parameters, has the advantage of being developed with the assistance of radical additions to styrenes⁴⁰ and affords a reasonable, albeit not fully satisfying, correlation ($\rho_{mb} = -0.22$, $\rho_{JJ}^* = 0.44$, $R^2 = 0.84$), establishing the importance of both polar (modest positive charge developing) and spin-delocalizing effects ($|\rho_{mb}/\rho_{JJ}^*| = 0.5$). Competitive NNs aziridination data [$\log(k_X/k_H)$] can be crudely correlated with the general σ_p scale, and the fit can be improved by employing the resonance-responsive σ^+ parameters ($R^2 = 0.93$ for σ^+ , 0.86 for σ_p), as expected. Marginal improvement is achieved by employing Jiang's dual-parameter approach ($\rho_{mb} = -0.42$, $\rho_{JJ}^* = 0.43$, $R^2 = 0.94$). The modest negative ρ_{mb} value (-0.42) is more pronounced than that obtained for NTs aziridinations, suggesting a more prominent positive charge developing en route to the transition state for the more electrophilic NNs moiety, whereas the much larger $|\rho_{mb}/\rho_{JJ}^*|$ ratio (0.98) confirms the predominance of polar over spin effects, more likely due to an early transition state.

Similar or higher polar over spin-delocalization effect values have been obtained in aziridination (NR) of *p*-substituted styrenes by Pérez's Tp^xM (M = Cu, Ag) systems²⁰ [$|\rho^+/\rho^*| = 0.925$ – 1.625 (NTs); ρ^* is associated with the Jackson⁴¹ spin-delocalization scale] and Che's [Ru(Por)(NSO₂R)₂] compounds^{17b,d} [$|\rho_{mb}/\rho_{JJ}^*| = 0.55$, 2.02 (NTs), 1.46 (NNs)], while

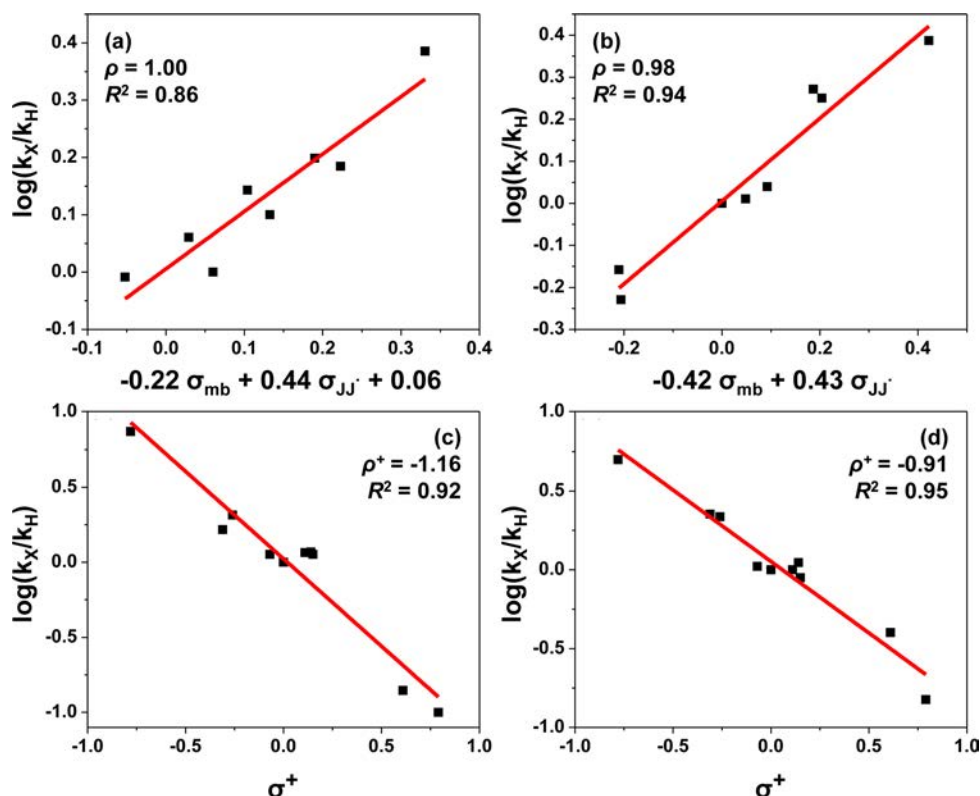


Figure 3. Top: Linear free energy correlation of $\log(k_X/k_H)$ vs $(\sigma_{mb}, \sigma_{JJ}^*)$ for aziridination of para-substituted styrenes catalyzed by (a) 1/PhI=NTs and (b) 1/PhI=NNs. Bottom: Linear free energy correlation of $\log(k_X/k_H)$ vs σ^+ for amination of para-substituted toluenes by (c) 1/PhI=NTs and (d) 1/PhI=NNs.

Betley's Fe^{II}-dipyrrinato complexes⁴² provide an unusually low $|\rho_{mb}/\rho_{JJ}^*|$ ratio of 0.04 (for NAd).

Incidentally, competitive aziridination of each para-substituted styrene (Table S7, SI) by equimolar amounts of PhI=NTs and PhI=NNs indicates that aziridinations by NNs are 2–7 times faster than those with NTs, in agreement with the anticipated electrophilic nature of the reactive oxidant.

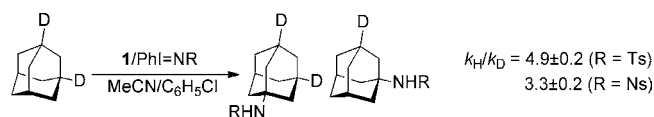
ii. Aminations. Hammett plots resulting from competitive amination reactions (followed by ¹H NMR) of a panel of nine para-substituted toluenes (4.0 mmol) vs toluene (4.0 mmol) by PhI=NTs or PhI=NNs (0.50 mmol) in the presence of **1** (0.050 mmol) in MeCN (Tables S8 and S9, SI) are shown in Figure 3 (bottom). Both NTs- and NNs-based aminations correlate reasonably well with σ_p and even better with σ^+ parameters [$R^2 = 0.92$ (NTs), 0.95 (NNs)], demonstrating significant development of positive charges [$\rho^+ = -1.16$ (NTs), -0.91 (NNs)], being slightly less pronounced for NNs, probably due to an earlier transition state. Application of the dual parameter approach leads to insignificant improvements (NTs, $\rho_{mb} = -1.19$, $\rho_{JJ}^* = 0.81$, $R^2 = 0.94$; NNs, $\rho_{mb} = -0.92$, $\rho_{JJ}^* = 0.30$, $R^2 = 0.95$), which, however, depict the large dominance of polar effects ($|\rho_{mb}/\rho_{JJ}^*| > 1$), as expected for a C–H bond scission reaction. The prototypical H atom abstraction from toluenes by the bromine atom, which is known to give rise to polar transition states,⁴³ provides Hammett correlations with similar ρ^+ values [-1.26 (40 °C), -1.17 (10 °C)].

More modest ρ^+ values (-0.47 ,^{13g} -0.55 ,^{13c} -0.66 ,⁴⁴ -0.73 ,^{13a} -0.90 ^{13f}) are obtained in Rh-based, apparently concerted, benzylic aminations, whereas more sizable values, similar to those obtained with **1**, are provided by the

structurally analogous $[\text{Ru}_2(\text{hp})_4\text{Cl}]$ ($\rho^+ = -0.90$) and $[\text{Ru}_2(\text{esp})_2\text{SbF}_6]$ ($\rho^+ = -1.49$),^{17a} reportedly operating via a stepwise mechanism. Surprisingly, data provided by Fe^{II}-dipyrrinato⁴² and Co(Por)^{15g} amination catalysts can only be correlated with the use of both polar and spin-delocalization parameters, featuring very low $|\rho_{mb}/\rho_{JJ}^*|$ values [0.358 (Fe), 0.008 (Co)].

b. KIE Measurements. i. Tertiary and Benzylic C–H Aminations. A primary deuterium kinetic isotope effect (KIE) for the tertiary C–H position was evaluated with the assistance of 1,3-*d*₂-adamantane ($96.7 \pm 0.2\%$ D₂), which was allowed to react in excess (1.3 equiv) with PhI=NTs or PhI=NNs (1.0 equiv) in the presence of **1** (0.1 equiv) in a mixture of MeCN/chlorobenzene (1:10 v/v) (Scheme 2). The KIE value

Scheme 2

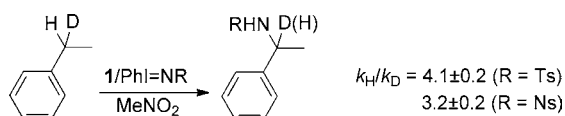


was assessed most consistently via ESI-MS, by extracting the ratio of sodiated $[d_2\text{-}t\text{-AdN(H)X} + \text{Na}]^+$ ($X = \text{Ts}, \text{Ns}$) vs $[d_1\text{-}t\text{-AdN(H)X} + \text{Na}]^+$, as well as the ratio of adamantyl fragments $[d_2\text{-}t\text{-Ad}]^+$ vs $[d_1\text{-}t\text{-Ad}]^+$ after cleavage of the amine moiety. After applying the necessary corrections⁴⁵ for (i) the isotopic natural abundance contribution of the *d*₁- to the *d*₂-containing ion and (ii) the fact that the substrate contains 3.3% of 1-*d*₁-adamantane, we arrive at a KIE of 4.9 ± 0.2 for NTs-based and 3.3 ± 0.2 for NNs-based adamantane aminations.

Nicholas has reported comparable KIE values for the metal-free, iodine-catalyzed amination of 1,3-*d*₂-adamantane by PhI=NTs (KIE = 5.12) and PhI=NNs (KIE = 2.68).⁴⁶ Müller has also reported a similar KIE value (3.5 ± 0.2) for the [Rh₂(OAc)₄]-catalyzed amination (PhI=NNs) of the same substrate.^{13f} Very limited KIE data are available for unactivated C–H bond amination by nitrene-transfer chemistry, the most prominent being those for the amination of cyclohexane/*d*₁₂-cyclohexane by Warren and co-workers' copper β-diketiminates/AdN₃ [KIE = 6.6(1)],^{12b} Huard and Lebel's [Rh₂(tpa)₄]/TrocnHOTs (KIE = 5),^{13g} and Che and co-workers' [Ru^{IV}(F₂₀-TPP)Cl₂]/N₃P(O)(OCH₂CCl₃)₂ (KIE = 5.1)^{17e} and [Fe(qpy)(MeCN)₂](ClO₄)₂/PhI=NTs (KIE = 4.8, 25 °C).^{14f}

The KIE for benzylic positions was assessed by virtue of the amination of 1-*d*-ethylbenzene (D1 = 97.4 ± 0.2%), under the conditions noted for adamantane, albeit in nitromethane (Scheme 3). The KIE values [4.1 ± 0.2 (NTs) and 3.2 ± 0.2

Scheme 3



(NNs)] were extracted from the H/D content of the benzylic position in the resulting amines (evaluated most consistently by ¹H NMR) and further corrected for the presence of 2.6% ethylbenzene. The observed KIE values encompass both primary and secondary effects [(k_H/k_D)_{obs} = (k_H/k_D)_{prim}(k_D/k_H)_{sec}]; hence, the true primary KIE value for the amination of benzylic C–H bonds may be somewhat higher. Under the reaction conditions of this KIE experiment, the desaturation and doubly tosylated byproducts (Table 1, entry 7) were not detected.

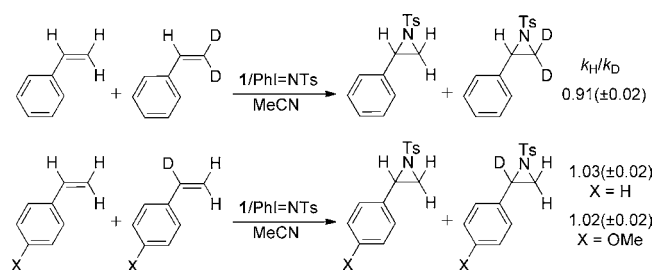
These KIE values are more modest than those reported for the amination of ethylbenzene/*d*₁₀-ethylbenzene by copper or nickel β-diketiminates/AdN₃ [KIE = 5.3(2),^{12b} 4.6(4)^{16a}], and stoichiometric [Ru^{VI}(Por)(NTs)₂] (KIE = 11)^{17d} or [Ru^{VI}(Por)(NNs)₂]/pyrazole (2% w/w) (KIE = 4.8).^{17b} A similarly high KIE value is obtained in Du Bois' [Ru₂(hp)₄Cl]-catalyzed intramolecular benzylic amination of PhCH(D)-CH₂OSO₂NH₂ combined with PhI(O₂C^tBu)₂ (KIE = 4.9 ± 0.2),^{17a} although the corresponding [Rh₂(OAc)₄]-catalyzed reaction provides a moderate KIE value (2.6 ± 0.2),^{13c,17a} consistent with a stepwise versus a concerted mechanism, respectively. Very large KIE values have also been reported for the amination of toluene/*d*₈-toluene by [Co^{II}(Por)]/NsN₃ (KIE = 14)^{15g} or Fe–dipyromethene/AdN₃ [KIE = 12.8(5)].^{14a} The copper-diimine catalyzed competitive amination of PhCMe₂H/PhCMe₂D by TsNNaCl gives a more modest KIE value (4.6),^{12c} whereas a Sc³⁺-stabilized Cu=NTs intermediate afforded a value of 5.1 with *d*₄-dihydroanthracene.^{21a}

The sizable KIE values reported here for aminations of *tert*-C–H and benzylic positions by **1** are consistent with C–H bond cleavage in the reaction mechanism. If we assume, as computational work suggests (see below), that C–H cleavage is also the turnover-limiting step, then concerted C–H bond activation is inconsistent with these high KIE values, and a two-step process, involving substrate-centered carboradical and/or carbocationic intermediates, may be a more likely scenario. As

anticipated, the KIE values are sensitive to the electronic nature of the nitrene moiety, with the more electrophilic NNs exhibiting significantly lower values, most likely due to an earlier transition state. Consequently, arguments attempting comparisons between literature-reported KIE values for aminations should take the electronic constitution of the NR group into account. Interestingly, Rh-catalyzed *tert*-C–H aminations afford similarly high KIE values (3.5–5.0).^{13fg} Hence, a distinction between concerted (for Rh) and two-step pathways (for all other elements, with some possible exceptions^{17g}) cannot be readily made on this evidence alone for *tert*-C–H sites.

ii. *Aziridinations*. Secondary KIE data (k_H/k_D) for aziridination reactions were collected with the assistance of suitably deuterated styrenes (Scheme 4). First, the β-styrene

Scheme 4

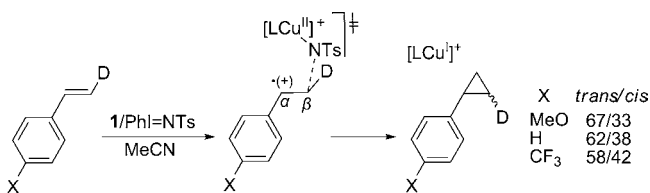


position was examined by virtue of the competitive aziridination (PhI=NTs, 0.25 mmol) of PhCH=CH₂/PhCH=CD₂ (1.0 mmol of each olefin), mediated by **1** (0.0125 mmol) in CH₃CN. An inverse KIE value ($k_H/k_D = 0.91 \pm 0.02$) was evaluated by ¹H NMR, suggesting N–C association between the electrophilic nitrenoid moiety and the β-styrene site in the transition state. The α-styrene position was then studied in a similar experiment involving PhCH=CH₂/PhCD=CH₂. A normal, albeit minute, KIE value of $k_H/k_D = 1.03 \pm 0.02$ was obtained, indicating that the α-olefinic site is unlikely to be engaged in the electrophilic phase of the nitrene addition to the olefin in tandem with the β-site (concerted, asynchronous NTs addition). The competitive addition of NTs to *p*-MeO-PhCH=CH₂/*p*-MeO-PhCD=CH₂ also furnishes a similar KIE value ($k_H/k_D = 1.02 \pm 0.02$) for an olefin that exhibits better retention of stereochemistry upon aziridination (see below). If anything, these miniscule KIE values might denote a slight α-D effect⁴⁷ with respect to the incipient C_α-centered radical or carbocation.

c. *Stereocontrol in Olefin Aziridinations*. The stereospecificity in the aziridination of olefins was further studied with the aid of three *trans*-deuterated para-substituted styrenes [(*E*)-*p*-X-C₆H₄CH=CHD; X = MeO, H, CF₃; 2 mmol] subjected to aziridination by PhI=NTs (0.25 mmol) in the presence of **1** (0.0125 mmol) in CH₃CN. The resulting aziridines were analyzed in situ by ²H NMR (and ¹H NMR) to provide the relative *cis/trans* deuterium content at the β-CHD position. The results (Scheme 5) show a small but discernible increase in stereospecificity with increasing electron-donor character of the para-substituent.

Incidentally, no isomerization of the remaining styrene is detected; hence, the aziridination step does not show signs of reversibility. In addition, no incorporation of deuterium in the α-C position is observed, suggesting that 1,2-H/D exchange is not operative. Assuming that the barriers for C_α–C_β bond

Scheme 5



rotation will not be much affected by the nature of the para-substituent, the observed trend is better accommodated by the presence of a dominant benzylic carboradical rather than a carbocation. The latter should be expected to suppress the rate of addition of the NTs moiety to the α -olefinic site with increasing electron-donor character of the para-substituent in the nucleophilic phase of a two-step mechanism. In contrast, recent work⁴⁸ has indicated that the barriers for the recombination of carboradicals with metal attached moieties are reduced for more-electron-rich radicals, since the barrier for the $3e^-$ bond formation ($N-C_\alpha$ in our case) is essentially dictated by the ease of oxidation of the carboradical.

d. Radical Trap and Clock Studies. i. CBrCl₃. In order to evaluate the evolution of the putative solvent-caged $\{[LCu-NHTs]^+/R^\bullet\}$ intermediate with respect to “in-cage” recombination vs radical diffusion in the solvent at large, the efficient carboradical trap CBrCl₃ ($R^\bullet + CBrCl_3 \rightarrow RBr + \bullet CCl_3$) was used in the amination of adamantane (0.25 mmol, 0.1 M) by **1** (0.025 mmol)/PhI=NTs (0.5 mmol) in chlorobenzene (2.5 mL). The concentration of CBrCl₃ was varied from 0.0 to 2.0 M, and the product profile (1-adamantyl-NHTs, 1-bromoadamantane, 1-chloroadamantane), along with the remaining adamantane, was quantified in situ by ¹H NMR spectroscopy. In these dilute solutions the yield of amination in the absence of CBrCl₃ is low (20%), but such solutions are necessary to assess the trapping of diffusively free radicals, since at high concentrations of CBrCl₃ (>0.1 M) the trap is expected to become an integral part of the solvent cage.⁴⁹

Figure 4 depicts the ratio of halogenated products (1-AdBr + 1-AdCl) over the amination product 1-AdNHTs, as a function of increasing concentration of CBrCl₃. The overall yield of the reaction with respect to adamantane remains within a narrow range (20 ± 2%) up to [CBrCl₃] = 1.6 M; lowering of the yield

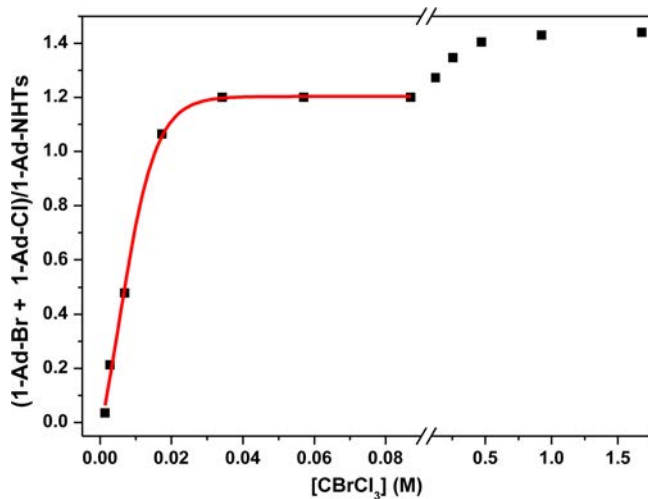


Figure 4. Ratio of halogenated (1-AdBr + 1-AdCl) over amination (1-AdNHTs) products vs the concentration of CBrCl₃.

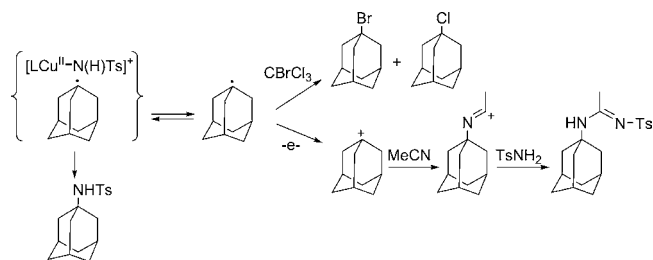
is observed thereafter. A plateau at (1-AdBr + 1-AdCl)/(1-AdNHTs) = 1.2 is quickly reached in the low CBrCl₃ concentration region (0.03–0.1 M). A gradual increase of the product ratio (approaching 1.5 at [CBrCl₃] = 1.6 M) is observed at higher concentrations of CBrCl₃. Interestingly, 1-AdCl supersedes 1-AdBr at very low CBrCl₃ concentration (<7.0 mM), but 1-AdBr rises rapidly at the expense of 1-AdCl at higher CBrCl₃ concentration (1-AdBr/1-AdCl = 10; [CBrCl₃] = 0.034 M). The reported 1-AdBr/1-AdCl ratio of 17⁵⁰ for capturing authentic adamantyl radicals is only reached at [CBrCl₃] = 0.5 M. Chloroform was not detected; hence, interference due to H atom abstraction by $\bullet CCl_3$ and initiation of a radical chain reaction is not anticipated.⁵¹

A dual plateau theory has been anticipated and partially observed in relation to cage effects associated with Co–C bond homolysis of adocobalamin and subsequent trapping of adenosyl radicals by TEMPO.^{49a} The use of TEMPO in our case produces a complicated product profile that points toward a multitude of side reactions. The plateau around 1.2 in Figure 4 can be reasonably interpreted as a reflection of an approximately 55:45 balance between diffusively free and caged-trapped 1-adamantyl radicals. As the concentration of CBrCl₃ increases above 0.1 M, the trap is anticipated to start inserting into the solvent-cage walls and thus initiate trapping of caged radicals in competition with radical rebound. Hence, the ratio of (1-AdBr + 1-AdCl)/(1-AdNHTs) is expected to rise, but as the overall product yield eventually starts curving downward at [CBrCl₃] ≥ 2.0 M, no further insights can be gleaned from the high CBrCl₃ concentration region. It is conceivable that metal/trap halogen-atom transfer chemistry ($Cu^I + CX_4 \rightarrow Cu^{II}-X + \bullet CX_3$; X = Br, Cl) may interfere at high CBrCl₃ concentration.

These results are also qualitatively consistent with observations in concentrated acetonitrile solutions, in a series of aminations of adamantane (0.25 mmol, 1.0 M) by **1** (0.025 mmol)/PhI=NTs (0.5 mmol) in acetonitrile (0.25 mL), to which variable concentrations of CBrCl₃ (≤1.0 M) were added. In the absence of CBrCl₃ the ratio of products of amidination over amination is 1.3. Addition of CBrCl₃ leads to progressive reduction of the amidination product in favor of 1-AdBr/1-AdCl, while the amination product remains largely unaffected. These results are consistent with the release of diffusively free 1-adamantyl radicals, which are subject to oxidation to the carbocation (precursor of the amidination product), most likely by Cu^{II} sites, in competition with trapping by CBrCl₃ (Scheme 6).³⁴

The ratio of in-cage/out-of-cage radical trapping will most likely depend on the substrate. Indeed, a preliminary series of experiments involving the amination of ethylbenzene in the presence of variable concentrations of CBrCl₃ affords a high ratio of PhCH(NHTs)CH₃/PhCHBrCH₃ (≥5.0). This may

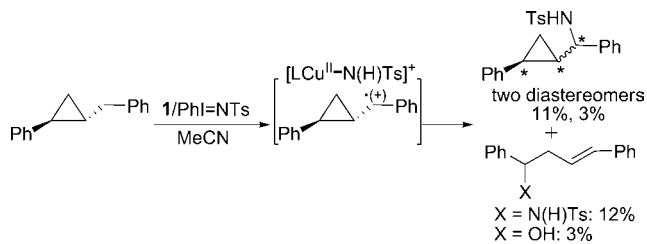
Scheme 6



explain why potentially carbocation-derived products (aziridine, amidine) in the amination of ethylbenzene (Table 1, entry 7) are obtained in low yields. In contrast, 2-methylbutane provides very little amination product (Table 2, entries 5 and 6), which suggests that the *tert*-radical precursor may largely be diffusively free.

ii. **Radical Clock.** Ingold's fast radical clock 1-benzyl-*trans*-2-phenylcyclopropane⁵² (1 equiv) was used in catalytic aminations (PhI=NTs, 2 equiv) mediated by **1** (0.1 equiv) in CH₃CN. The product profile obtained (Scheme 7) includes both ring-opened and ring-closed products in low yields.

Scheme 7



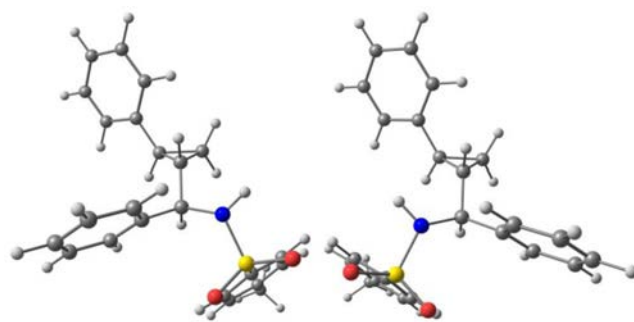
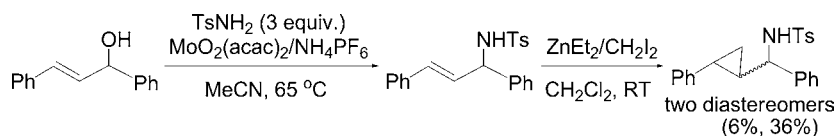
The ring-opened products are known *E*-olefins⁵³ and were identified by ¹H NMR with the assistance of authentic samples. The alcohol presumably results from capturing of the ring-opened radical or carbocation by residual water. Scrupulous exclusion of water reduces the alcohol to trace amounts and increases the amount of the amine, indicating competition for capturing the ring-opened electron deficient site, most likely a carbocation. The radical clock does not distinguish between an initially generated ring-closed benzylic radical or carbocation; hence, a ring-opened carbocation can either result from the rearrangement of a ring-closed carbocation, or, more likely, via oxidation of a diffusively free ring-opened radical.

The ring-closed products of benzylic amination are isolated as diastereomers (3.7:1) that can be separated and purified as oils by TLC. They have been identified with the assistance of authentic samples, prepared by cyclopropanation of the known precursor allylic amine⁵⁴ with the Wittig–Furukawa reagent Zn(CH₂I)₂.⁵⁵ Interestingly, the zinc reagent provides the diastereomers in the inverse ratio of 1:6 (Scheme 8).

COSY, HMQC, and HMBC NMR data have been collected to assist in assigning all proton and carbon atoms (Figures S12–S15 and S17–S21, SI), and NOESY spectra (Figures S16 and S22, SI) have been obtained to facilitate the stereochemical assignment of the two isomers (Figure S11 and Table S10, SI) in conjunction with calculated structures (Figure 5). The best fit affords *SSR*/*RRS* (major) and *SSS*/*RRR* (minor) assignments for the three stereocenters (from left to right in Scheme 7) of the diastereomers produced by the Cu-mediated amination.

The same radical clock has been used by Barman et al.^{12c} in a similar Cu^I-mediated NTs-insertion reaction. Both ring-opened *E*/*Z*-olefinic amines and the closed-ring amination product (as

Scheme 8

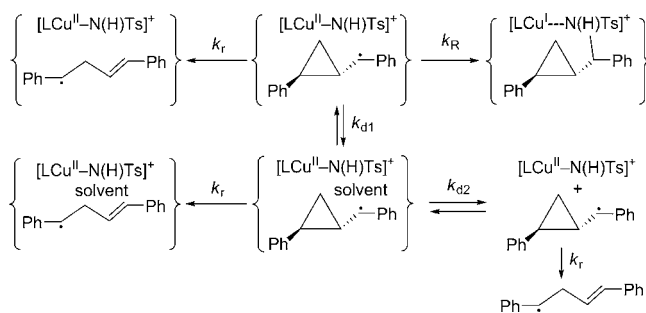
Figure 5. B3LYP/6-311+G(2d,p)-optimized structures of *SSR*/*RRS* (left) and *SSS*/*RRR* (right) isomers.

a single compound⁵⁶) were isolated. More recently, Warren and co-workers have also applied the same radical clock in a dicopper–nitrene [Cu₂(μ-N^tBu)]-mediated amination, yielding only the ring-opened olefinic amination product.^{12a}

Given that the benzylic radical, generated by H atom abstraction, has been calibrated by Ingold and co-workers⁵² to ring-open with a rate constant of $k_r = (3.6 \pm 0.5) \times 10^8 \text{ s}^{-1}$ at 40 °C (or approximately $2.0 \times 10^8 \text{ s}^{-1}$ at room temperature) and that the ratio of ring-opened to ring-closed products in the present experiments is 1.07:1, we estimate that the apparent rate constant for the incipient radical/carbocation recombination (k_R) with the putative [LCu–N(H)Ts]⁺ moiety would be of similar magnitude ($k_R \approx 1.9 \times 10^8 \text{ s}^{-1}$, at room temperature). The apparent radical/carbocation lifetime ($\tau = 1/k_R$) would thus be in the vicinity of 5 ns. It is unlikely that the ring-opened and ring-closed products represent parallel stepwise and concerted amination mechanisms, respectively, since there is no other evidence supporting a concerted NTs-insertion pathway.

The radical clock kinetics is predicated on the assumption that the competition between radical-pair recombination (k_R) and rearrangement (k_r) is taking place in the absence of other interfering factors (Scheme 9, top line). However, following an

Scheme 9



argument made by Groves and co-workers,⁵⁷ if the solvent-caged radical pair is also susceptible to cage escape via solvent-separated radical-pair dissociation (k_{d1}) and eventually out-of-

cage diffusion (k_{d2}), as the aforementioned experiments with CBrCl_3 suggest (although to a limited extent for ethylbenzene), then the experimentally deduced radical recombination rate constant (k_R) may be underestimated. Indeed, in a hypothetical scenario in which the rate constants for radical-pair recombination (k_R) and cage escape (k_d) are about equal and at least an order of magnitude above the rate constant for radical rearrangement (k_r), then the experimentally derived ratio of ring-opened vs ring-closed products will largely reflect the competition between radical-pair recombination vs cage escape.

e. Metal- and Ligand-Centered Events. i. Variable-Temperature ESI-MS (VT-MS) Data. Variable-temperature, cryospray-ESI-MS (VT-MS)⁵⁸ spectra have been obtained from acetonitrile solutions of **1** and $\text{PhI}=\text{NTs}$ (variable ratios; Figures 6 and S23–S25, S1), initially mixed at low temperature

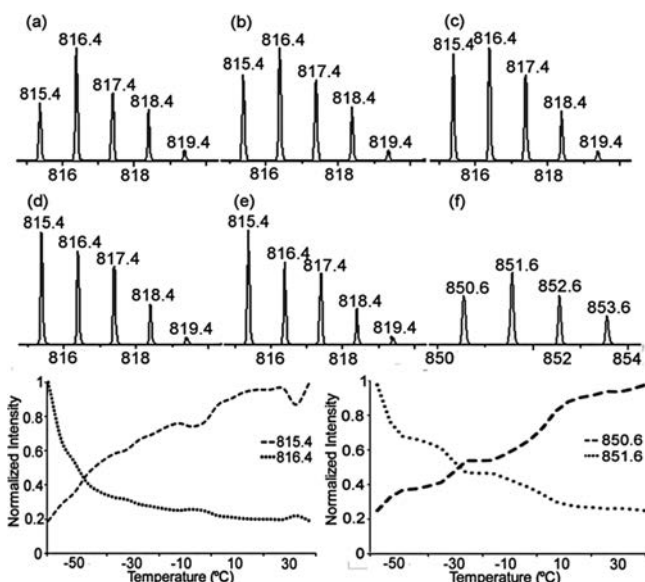


Figure 6. Top: VT-MS spectra from reaction of **1** and $\text{PhI}=\text{NTs}$ (1:0.75) in MeCN at -50°C and different time intervals, (a) 1.5–2.0 min, (b) 2.0–2.5 min, (c) 2.5–3.0 min, (d) 3.0–3.5 min, (e) 3.5–4.0 min, and from reaction of $1\text{-}d_{36}$ and $\text{PhI}=\text{NTs}$ (1:0.5) in MeCN at -50°C for (f) 1.5–2.0 min. Bottom: (Left) Decay of m/z 816.4 and buildup of m/z 815.4 as a function of temperature ($1/\text{PhI}=\text{NTs}$, 1:0.75). (Right) Decay of m/z 851.6 and buildup of m/z 850.6 as a function of temperature ($1\text{-}d_{36}/\text{PhI}=\text{NTs}$, ≤ 1 equiv vs $1\text{-}d_{36}$) in MeCN.

(-50°C) and sampled after 30–60 s of stirring. Although the cation of **1** ($m/z = 647.4$) dominates, small discernible features of other cations become apparent. Key among them is the cluster of peaks starting at $m/z = 815.4$, which contains at least two species ($m/z = 815.4$ and 816.4 ; Figure 6a). The 816.4 ion can be better detected with substoichiometric amounts of $\text{PhI}=\text{NTs}$ vs **1** (ratios ranging from 0.5:1 to 1:1). Most importantly, a series of spectra obtained as a function of time at constant temperature (Figure 6a–e) indicate gradual loss of the 816.4 cation with concomitant buildup of the 815.4 cation. In addition, the same trend is observed as a function of raising the temperature from -50 to 30°C , correlating reasonably well with a direct conversion of cation m/z 816.4 to 815.4 (Figures 6 (bottom) and S26, S1). The m/z 815.4 cation is stable at room temperature and has been isolated from large-scale reactions of **1** and $\text{PhI}=\text{NTs}$ (3 equiv) in CH_3CN as Cu^{II}

Scheme 10

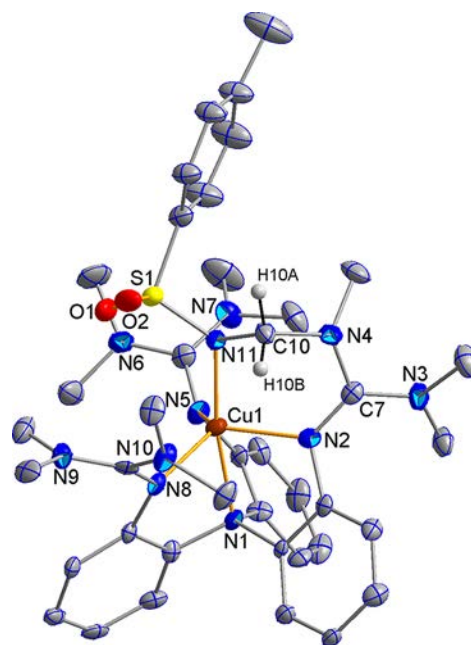
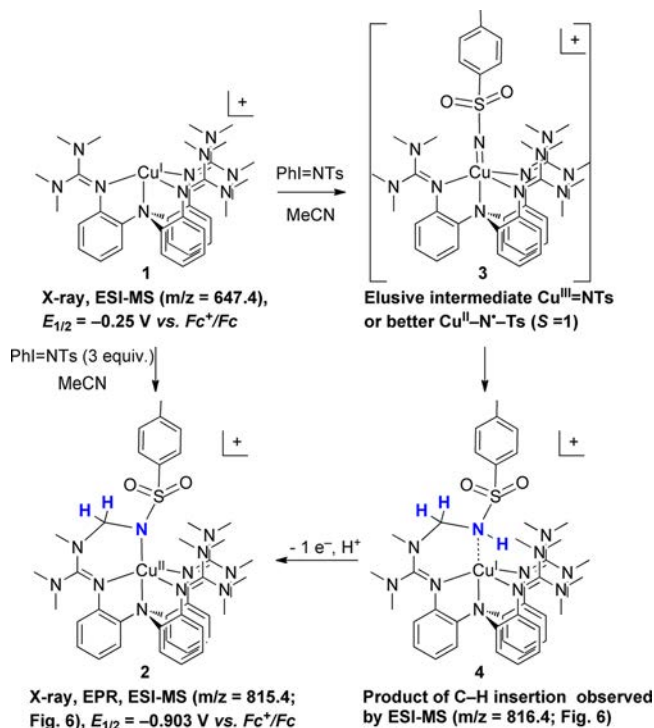


Figure 7. ORTEP diagram of **2** (cation only) drawn with 40% ellipsoids. Selective interatomic distances (Å) and angles (deg): $\text{Cu}(1)\text{-N}(1) = 2.073(7)$, $\text{Cu}(1)\text{-N}(2) = 2.092(7)$, $\text{Cu}(1)\text{-N}(5) = 2.119(7)$, $\text{Cu}(1)\text{-N}(8) = 2.027(7)$, $\text{Cu}(1)\text{-N}(11) = 1.960(7)$; $\text{N}(11)\text{-Cu}(1)\text{-N}(1) = 169.9(3)$, $\text{N}(11)\text{-Cu}(1)\text{-N}(2) = 105.7(3)$.

species **2** (Scheme 10, Figure 7, Table S1, S1), featuring insertion of NTs into the C–H bond of a ligand Me group. Similar ligand-centered insertions have been observed in metal–oxo^{24b,59} and metal–nitrene chemistry.^{14i,15i,60} Notably, species **2** is one oxidizing equivalent above the $1/\text{PhI}=\text{NTs}$ level. A similar compound (Figure S2, Table S1, S1) has been obtained from $1/\text{PhI}=\text{NSO}_2\text{Ph-p-MeO}$.

The identity of the cation with m/z 816.4 is more challenging and could include (i) the elusive $[\text{LCu}=\text{NTs}]^+$ oxidant **3**; (ii) the Cu^{I} species **4**, i.e., the initial product of NTs ligand-insertion at the same oxidation level as $1/\text{PhI}=\text{NTs}$; and (iii) a combination of **3** and **4** (Scheme 10). To distinguish among these possibilities, the perdeuterated-methyl analog $[\text{Cu}^{\text{I}}(\text{d}_{36}\text{-TMG}_3\text{trphen})][\text{PF}_6]$ (**1-d₃₆**) was synthesized and examined by variable-temperature (VT) cryospray-ESI-MS in combination with $\text{PhI}=\text{NTs}$ (≤ 1 equiv vs **1-d₃₆**; Figures 6f and S27, SI). The cluster of peaks starting at m/z 850.6 is the deuterium analog of the all-protio m/z 815.4 cluster noted above and reveals again the presence of at least two ions (m/z 850.6 and 851.6). The m/z 850.6 ion confirms the identity of the corresponding all-protio 815.4 ion as the NTs ligand-inserted compound **2-d₃₅**. However, the m/z 851.6 ion, which decays in exactly the same time- and temperature-dependent manner as the all-protio 816.4 ion (Figure 6, bottom), is *not* consistent with the deuterated version of **3** ($m/z = 852.6$, **3-d₃₆**) but rather with **4** ($m/z = 851.6$, **4-d₃₅**), featuring an N–H bond, probably due to quick H/D exchange. However, the isotopic pattern cannot exclude the presence of **3-d₃₆** as a minor component. These results suggest that the reaction pathway observed in the $1/\text{PhI}=\text{NTs}$ system is the generation of **4** via ligand-centered NTs insertion (Scheme 10) and its conversion to **2** via a formal one-electron oxidation, coupled to deprotonation (or an equivalent hydrogen-atom abstraction).

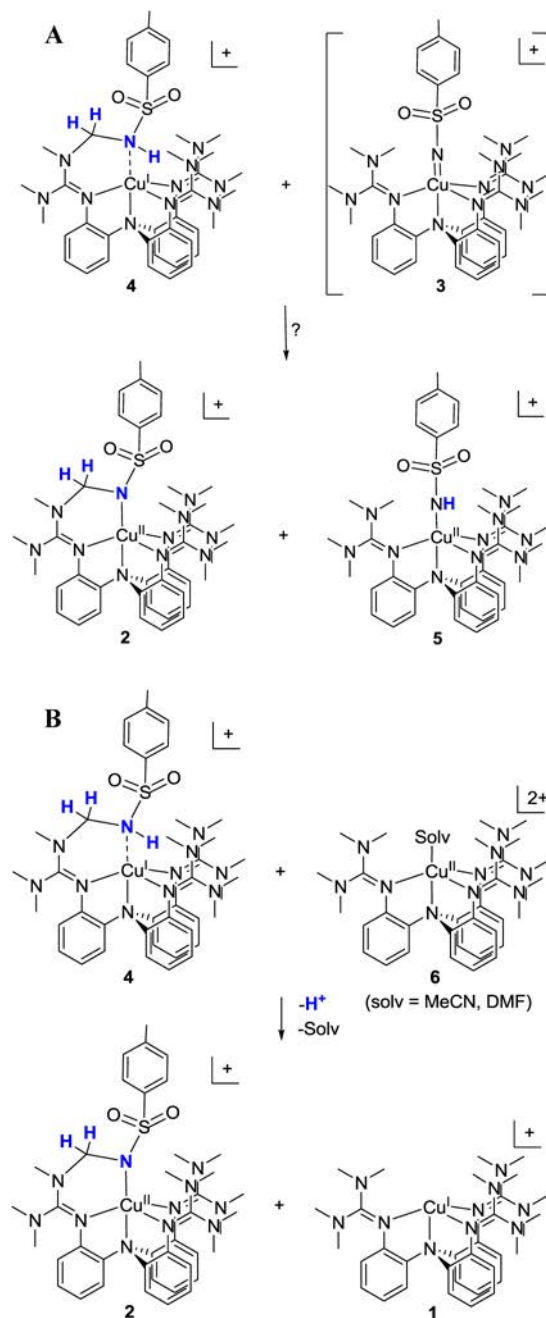
Which species serves as the one-electron oxidant? By analogy to similar ligand-based oxo insertions studied by Que and co-workers,^{24b} we first entertained the possibility that the elusive $[\text{LCu}=\text{NTs}]^+$ (**3**) might be responsible for the oxidation of **4** to **2** via H atom transfer (comproportionation reaction; Scheme 11A), giving rise to $[\text{Cu}^{\text{II}}\text{-N(H)Ts}]^+$ amide (**5**). However, formation and/or decay of **5** (m/z 817.4) has *not* been observed by means of VT-MS; hence, the operation of this reaction scheme is questionable, unless **5** is highly reactive.

An alternative hypothesis is that $[\text{Cu}^{\text{II}}(\text{TMG}_3\text{trphen})]^{2+}$ (**6**) might serve as the oxidant (Scheme 11B). This Cu^{II} ion is detected in $1/\text{PhI}=\text{NTs}$ solutions by ESI-MS [as the 2+ ion ($m/z = 323.7$) and as $[\text{Cu}^{\text{II}}(\text{TMG}_3\text{trphen})(\text{Cl})]^+$ ($m/z = 682.3$) in combination with incident chloride in the MS cavity], as well as by means of electrochemical and EPR data (see below). The Cu^{II} compound **6** has been prepared independently by one-electron oxidation of **1** by AgPF_6 in MeCN and has been crystallographically characterized (Figure S1 and Table S1, SI) as the five-coordinate $[\text{Cu}^{\text{II}}(\text{TMG}_3\text{trphen})(\text{MeCN})][\text{PF}_6]_2$. Although the exact provenance of **6** in the reaction chemistry of $1/\text{PhI}=\text{NTs}$ is not yet known, it is reasonable and thermodynamically feasible (see electrochemical data below) to suggest that the oxidation of **4** may be due to $[\text{Cu}^{\text{II}}(\text{TMG}_3\text{trphen})]^{2+}$ (**6**), generating the NTs-inserted product **2** and $[\text{Cu}^{\text{I}}(\text{TMG}_3\text{trphen})]^+$ (**1**) (Scheme 11B).

A few other ESI-MS-derived observations are potentially relevant to the operation of the $1/\text{PhI}=\text{NTs}$ system. Assignments were made with the assistance of parallel **1-d₃₆**/ $\text{PhI}=\text{NTs}$ experiments. First, not only is the single NTs insertion product **2** observed but also very small amounts of the double ($m/z = 984.4$) and even a trace of the triple ($m/z = 1153.4$) NTs-insertion product, presumably involving successive insertions into the other two guanidinyll arms. These multiple insertions suggest that the precursor Cu^{I} species **4** may be capable of sustaining further nitrene-transfer chemistry.

Second, ESI-MS analyzed solutions of $1/\text{PhI}=\text{NTs}$ mixtures show that the Cu species that have undergone NTs insertion(s)

Scheme 11



into ligand NCH_3 moieties are also accompanied by copper-containing fragments ($m/z = 633.4, 801.4, 970.4$) that indicate loss of TsNCH_2- groups, effectively resulting in ligand demethylation ($-\text{N}-\text{CH}_3 + \text{“NTs”} \rightarrow -\text{N}-\text{CH}_2\text{NHTs} \rightarrow -\text{N}-\text{H} + \text{“TsNCH}_2\text{”}$). It is possible that these species represent gas-phase fragmentation chemistry under the ESI-MS voltage, since even pure **2** is attended by the demethylated congener. Nevertheless, by analogy to the observations in entry 16 (Table 1), $\text{R}_2\text{N}-\text{CH}_2-\text{NHTs}$ are inherently unstable toward products of N-demethylation. Indeed, the TsNCH_2 fragment can be captured during chromatographic purification of catalytic reaction mixtures of $1/\text{PhI}=\text{NTs}$ as the isolable product $\text{TsN(H)}-\text{CH}_2-\text{NHTs}$ (Figure S28, SI). The corresponding $\text{TsN(H)}-\text{CD}_2-\text{NHTs}$ has been obtained from **1-d₃₆**/ $\text{PhI}=\text{NTs}$ in CH_3CN , confirming that the source of methylene is

ligand-derived. However, we have not been able to observe this product in situ; hence, it is unclear whether *N*-demethylation, a well-known occurrence in catalytic oxygenation chemistry,³¹ is actually taking place in solution or is the result of postreaction analysis (ESI-MS voltage, chromatography column).

ii. Cyclic Voltammetry. Cyclic voltammetry of 1/PhI=NTs mixtures in MeCN at room temperature as a function of time (Figure 8) indicate a decrease of Cu^I (1) ($E_{1/2} = -0.267$ V vs

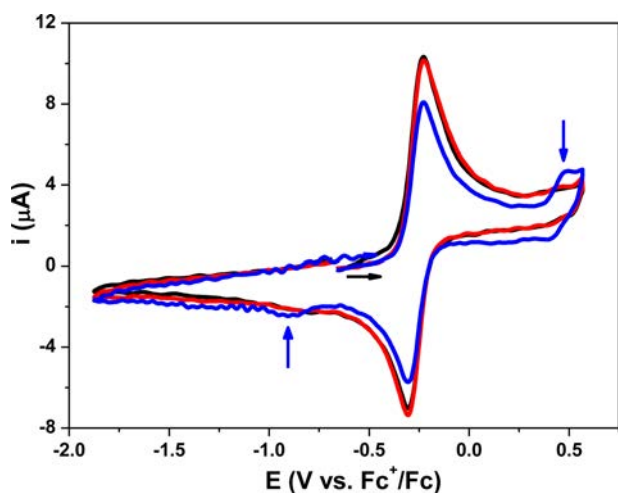


Figure 8. Cyclic voltammograms of 1/PhI=NTs (1:1 mixture) in MeCN/(ⁿBu₄N)PF₆, with a Au disk electrode (1.6 mm in diameter); scan rate 0.1 V/s. Black line, before addition of PhI=NTs; red line, 1 min; blue line, 5 min after the addition. The black arrow indicates the direction of the scan. Vertical arrows indicate the waves assigned to 2.

Fc⁺/Fc, evaluated with authentic 1; Figure S29, SI) within the first few minutes into the reaction, potentially in favor of Cu^{II} (6, evaluated with authentic 6; Figure S30, SI), with progressive development of the characteristic semireversible wave due to 2 ($E_{1/2} = -0.903$ V vs Fc⁺/Fc, evaluated with authentic 2; Figure S31, SI). Most notably, the potentials of the 1/6 and 2/4 redox couples indicate that the aforementioned oxidation reaction is thermodynamically feasible by a significant margin.

iii. EPR Spectroscopy. As expected for Cu^I complexes, frozen solutions of 1 in DMF or MeCN are EPR silent (not shown). EPR data were collected at temperatures in the vicinity of 20 K (as specified in Figure 9) on samples retrieved periodically (1–20 min) from the reaction of 1/PhI=NTs (1:1), conducted at –50 °C in DMF (as well as at –30 °C in MeCN). Close examination of spectra indicated that they consist of two overlapping signals, representing two different monomeric Cu^{II} species at no more than 10% of total Cu, in agreement with ESI-MS data that observe Cu^I species 1 as the dominant ion.

A representative spectrum recorded from a sample collected at 8 min is shown in Figure 9 (left, black), along with the contributing EPR signals for the two Cu^{II} species (Figure 9, left, red and green). These have been extracted with the assistance of spectra recorded on samples retrieved at different time intervals, showing variable contributions of the two signals. The Cu^{II} signal shown in red corresponds reasonably well with the EPR signal obtained from a frozen DMF solution of authentic complex 2 (Figure 9, right). Simulation parameters for complex 2 ($g_{\parallel}, g_{\perp}, g_3 = 1.995, 2.153, 2.243$; $|A_{\parallel}|, |A_{\perp}|, |A_3| = 229, 238, 248$ MHz) conform to a d_{z^2} ground state, as expected for a trigonal bipyramidal geometry with $g_{\parallel} = g_{\perp}$ (~ 2.00) < g_{\perp} . The signal shown in green is consistent with that obtained from a frozen

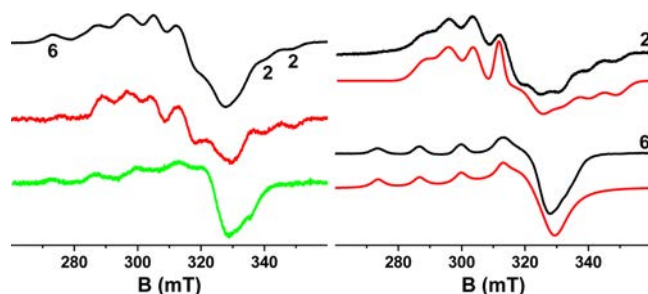


Figure 9. Left: Experimental X-band EPR spectrum from a sample retrieved at 8 min from the reaction of 1/PhI=NTs (1:1) at –50 °C in DMF (black). The numbers indicate the position of nonoverlapping signals attributed to complexes 2 and 6. Individual contributions of signals due to 2 (red) and 6 (green), respectively. Right: Experimental (black) and theoretical (red) spectra from frozen DMF solutions of 2 and 6. EPR conditions: T , 20 K (left) or 23 K (right); microwave power, 2 mW; modulation amplitude, 10 (left) or 5 (right) G_{pp}; microwave frequency, 9.41 GHz.

DMF solution of authentic complex 6 (Figure 9, right). The signal due to 6 is characterized by axial properties with $g_{\parallel} > g_{\perp}$ and $A_{\parallel} > A_{\perp}$ with the following parameters: $g_{\parallel}, g_{\perp,1}, g_{\perp,2} = 2.292, 2.083, 2.053$; $|A_{\parallel}| = 420$ MHz, $|A_{\perp,1}|, A_{\perp,2} \sim 50$ MHz. Efforts to identify any $S = 1$ species, potentially due to the elusive [LCu=NTs]⁺ intermediate 3, have not been successful. Notably, a recent study on detectable Cu^{II}–NTs intermediates assigns diamagnetic character to these species.^{21a}

In summary, ESI-MS, electrochemical, and EPR data lead to the conclusion that the major observable species in solutions of 1/PhI=NTs are predominantly 1, accompanied by small amounts of its redox partner [Cu^{II}(TMG₃trphen)]²⁺ (6) and modest amounts of the NTs-inserted redox couple 2/4.

3. Computational Studies. *a. Calculated Ground-State Cu^I Reagents.* Three variations of Cu^I catalysts were calculated with X = Me (1), H (1-H), and CH₂–NHTs (1-CH₂–NHTs) (Figure 10, top). The former represents the intact catalyst 1, and the other two denote potential in situ modifications of 1 as noted in the ESI-MS section. Similar Cu–N_{equatorial} (N2, N3, N4 in Figure 10) bond distances were calculated for the singlet ground states, with all being between 2.00 and 2.04 Å. The Cu–N_{axial} (N1) distance was calculated to be 2.21 Å in each of the three catalyst variations, somewhat shorter than in the solid-state crystal. Copper had Mulliken atomic charges of 0.51, 0.47, and 0.49 e[–], respectively, for 1, 1-H, and 1-CH₂–NHTs.

b. Computed Nitrene Intermediates. Upon ³NTs ligation (Figure 10, bottom), the B3LYP/6-31G(d)-calculated copper Mulliken atomic charges increased to 0.75, 0.76, and 0.75 e[–], respectively, for 1, 1-H, and 1-CH₂–NHTs. The unrestricted Kohn–Sham formalism was used, and the computed spin density places ~ 1 unpaired e[–] on the nitrene nitrogen and $\sim 2/3$ unpaired e[–] on Cu, with the remainder spread over other atoms (Figure S32, SI). Interestingly, upon ligation of ³NTs, one of the Cu–N_{equatorial} bonds in each structure is lengthened to distances ranging from 2.81 to 3.03 Å. Concomitantly, the Cu–N_{axial} distance is shortened upon formation of the nitrene intermediate, ranging from 2.08 to 2.11 Å. As expected, the Cu–NTs distance was calculated to be the shortest among all other Cu–N bonds [1.84 Å (1), 1.91 Å (1-H), 1.83 Å (1-CH₂–NHTs)], albeit somewhat longer than that reported for terminal copper–nitrene moieties.^{21b} Optimized [Cu]–N–Ts bond angles were calculated to be 135° (1), 127° (1-H), and 142° (1-CH₂–NHTs).

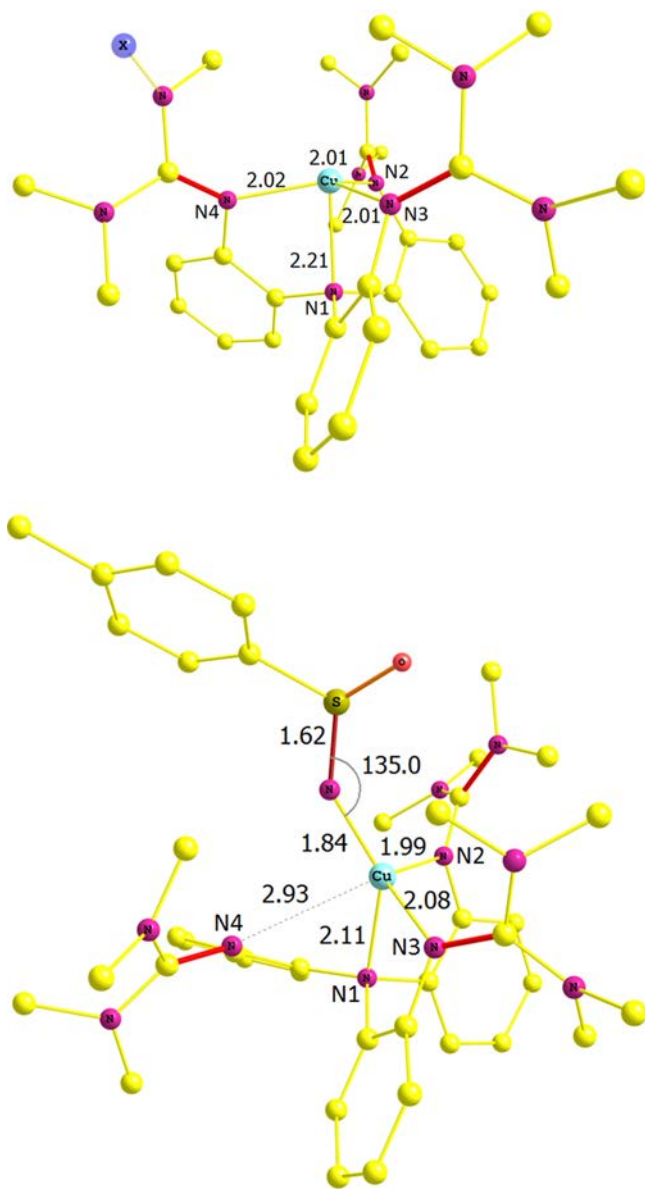


Figure 10. Compound **1** (top), with X denoting the location in which variations were modeled, and triplet nitrene $^3[\text{Cu}]\text{NTs}$ (bottom), with selected bond distances (Å) and angles (deg), for X = Me. Hydrogens are omitted from the figure for ease of viewing.

Upon nitrene binding, the singlet state of the [Cu] catalyst models changes to a triplet ground state for [Cu(NTs)]. Note that attempted isolation of the PhI=NTs adduct of complex **1** resulted in PhI dissociation upon geometry optimization. Attempts to find a $\kappa^2\text{-N,O}$ -nitrene-bound NTs resulted in rearrangement to the κ^1 linkage isomer shown in Figure 10 (bottom). The computed ΔG 's indicated that NTs ligation is exergonic by 23 kcal/mol (**1**), 27 kcal/mol (**1-H**), and 19 kcal/mol (**1-CH₂NHTs**). The ΔG difference between the corresponding singlet $^1[\text{Cu}]\text{NTs}$ and triplet $^3[\text{Cu}]\text{NTs}$ was 16 kcal/mol (**1**), 14 kcal/mol (**1-H**), and 20 kcal/mol (**1-CH₂NHTs**); hence, the singlet copper–nitrene is substantially destabilized vs the triplet ground state. Bond lengths and difference of lengths of singlet and triplet nitrene [Cu]NTs (X = Me) are given in Table S11 (SI).

Shown in Figure 11 are two of the more revealing frontier molecular orbitals (SOMOs) for $^3[\text{Cu}]=\text{NTs}$. Other frontier

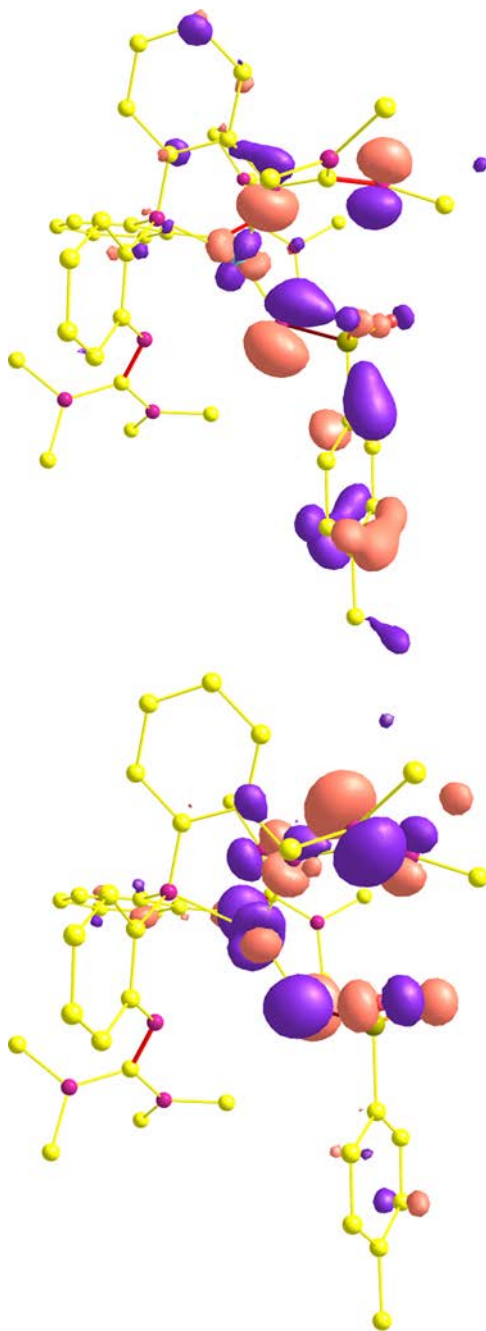
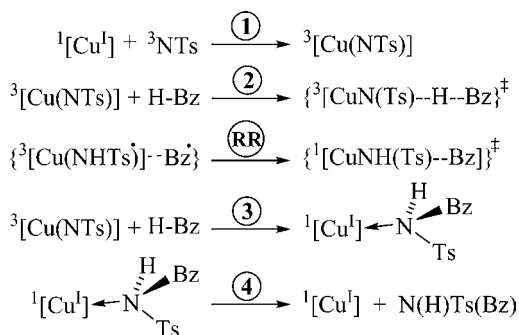


Figure 11. Important frontier α -SOMOs for triplet [Cu]=NTs. Contour value = 0.045. Hydrogens are omitted from the figure for ease of viewing. Yellow = carbon, magenta = nitrogen.

orbitals with significant copper–nitrene character are collected in the Supporting Information along with the computed spin densities (Figures S33–S35, SI). What is of interest is the delocalization of the density from the copper–nitrene active site to the sulfonyl, *p*-tolyl, and TMG₃trphen moieties. Given the present results, in conjunction with previous studies of the bonding of heterosubstituted nitrenes⁶¹ and aryl nitrenes,⁶² it is reasonable to conclude that delocalization stabilizes the putative nitrene intermediate enough to make it energetically accessible, but not so much as to quench its reactivity for group transfer. Furthermore, the greater activity of Cu=N–alkyl or Cu=N–SO₂R vs Cu=N–aryl complexes highlights the importance of

Table 5. B3LYP/6-31G(d)-Computed ΔG and ΔG^\ddagger Values (kcal/mol) for the Steps Shown in Scheme 12

X	step 1	step 2	RR	step 3	step 4
H	-27	25		-9	-17
CH ₃	-23	29	2	-6	-25
CH ₂ -NHTs	-19	26		-8	-27

Scheme 12

nitrene substituents in modulating the group transfer reactivity of the active species.^{12b}

c. Amination-Related Calculations. The amination of toluene by $^3[\text{Cu}]\text{NTs}$ was calculated (Table 5 and Scheme 12) to have activation barriers for benzylic C–H bond activation of $\Delta G^\ddagger = 29$ kcal/mol (**1**), 25 kcal/mol (**1-H**), and 26 kcal/mol (**1-CH₂NHTs**) relative to separated triplet copper–nitrene complex and toluene reactant; the transition states for toluene C–H activation (H atom abstraction) were calculated to be a triplet. The majority of the spin density resides on Cu ($0.7 e^-$), the nitrene N ($0.6 e^-$), and the benzylic C of toluene ($0.4 e^-$). The barrier was also computed using the BP86 functional, yielding $\Delta G^\ddagger = 35$ kcal/mol (**1**), 29 kcal/mol (**1-H**), and 31 kcal/mol (**1-CH₂NHTs**). Hence, BP86 values are commensurate with those obtained with B3LYP in terms of catalyst ordering, being consistently higher by ~ 5 kcal/mol. A comparison of BP86 and B3LYP for the $^3[\text{Cu}]\text{NTs}$ intermediate for **1**, **1-H**, and **1-CH₂NHTs** is shown in Table S12 (SI); the H atom abstraction transition state (TS) geometries are likewise similar.

Notably, the ^3TS for benzylic H atom abstraction from toluene was lower in energy by ~ 12 kcal/mol than the corresponding ^1TS for all three catalyst variants modeled. Following the intrinsic reaction coordinate (triplet surface) from $^3[\text{Cu}]\text{NTs}$ (for **1**) in the reactant direction showed its immediate precursor to be a weakly bound adduct of toluene and $^3[\text{Cu}]\text{NTs}$. The computed ΔG for the formation of this adduct from toluene and $^3[\text{Cu}]\text{NTs}$ is 8 kcal/mol. Computing the intrinsic reaction coordinate in the product direction (triplet surface) indicated formation of a $^3\{[\text{Cu}]\text{--NHTs}\cdots\text{CH}_2\text{Ph}\}$ caged adduct intermediate ($\Delta G_{\text{rel}} = +4$ kcal/mol; Scheme 13 and Figure 12).

A *constrained* optimization (singlet) for the radical rebound (RR) step showed $\Delta G^\ddagger = 2$ kcal/mol relative to the caged adduct. The *constrained* triplet was calculated to be 26 kcal/mol higher than that of the *constrained* singlet, suggesting that the spin-flip occurs before the TS for radical rebound. A kinetic penalty must presumably be paid for the singlet–triplet spin-flip. Finally, we note that $^3\{[\text{Cu}]\text{--NHTs}\cdots\text{CH}_2\text{Ph}\} \rightarrow ^1[\text{Cu}^1]\text{N(H)Ts(Bz)}$ is 10 kcal/mol exergonic. Dissociation of the radical pair, $^3\{[\text{Cu}]\text{--NHTs}\cdots\text{CH}_2\text{Ph}\} \rightarrow ^2[\text{Cu}^{\text{II}}]\text{N(H)Ts} +$

^2Bz , is 7 kcal/mol exergonic. The reaction coordinate is summarized in Scheme 13. These calculations thus imply a two-step amination sequence, H atom abstraction followed by radical rebound, as opposed to a single-step insertion.

The transformation $^3[\text{Cu}]\text{NTs} + \text{toluene} \rightarrow ^1[\text{Cu}^1]\text{N(H)Ts(Bz)}$ was *exergonic* by 6 kcal/mol (**1**), 9 kcal/mol (**1-H**), and 8 kcal/mol (**1-CH₂NHTs**) to form the singlet Cu^{I} –amine adduct, $[\text{Cu}^{\text{I}}]\text{N(H)Ts(Bz)}$. The last step in Scheme 13 is the amine dissociation, which was computed to be exergonic by 25 kcal/mol (**1**), 17 kcal/mol (**1-H**), and 27 kcal/mol (**1-CH₂NHTs**), reflecting the extreme steric crowding in the amine adduct and the favorable entropic contribution of ligand loss. The overall thermodynamics for nitrene insertion, $^3[\text{Cu}]\text{NTs} + \text{H-Bz} \rightarrow ^1[\text{Cu}^1] + \text{N(H)Ts(Bz)}$, was thus computed to be exergonic by 31 kcal/mol (**1**), 26 kcal/mol (**1-H**), and 35 kcal/mol (**1-CH₂NHTs**). Hence, the computations imply that, after the initial H atom abstraction to form a radical pair, namely, Cu^{II} –amide and benzyl radical, a radical rebound step occurs to give separated catalyst and amine product.

For the radical clock reaction shown in Scheme 7, from the separated reactants to a triplet TS for H atom abstraction, the B3LYP/6-31G(d) computed $\Delta G^\ddagger = 28$ kcal/mol. This barrier resembles that computed for H atom abstraction of toluene (Scheme 13). Thus, the cyclopropyl substrate must presumably go through a similar two-step process (H atom abstraction followed by radical rebound), which is consistent with the experimentally observed ring-opening of this radical-clock substrate.

d. Catalytic Aziridination Calculations. The aziridination of styrene was investigated with the model catalyst **1**. The optimized triplet TS is depicted in Figure 13A. What is particularly noticeable is the asymmetry of the C \cdots N bonds between the nitrene nitrogen and the vinyl carbon atoms; $C_\beta\cdots\text{N}_{\text{Ts}} = 2.31$ Å, $C_\alpha\cdots\text{N}_{\text{Ts}} = 3.10$ Å. Hence, the aziridination transition state geometry appears decidedly asynchronous with respect to the formation of the two carbon–nitrogen bonds. The geometry of the TS, in conjunction with the experimental data in Table 3, thus raises the question of whether the aziridination is concerted or not, as does the inference from the toluene amination computations, which suggest a two-step (H atom abstraction followed by RR) rather than one-step (direct insertion, albeit asynchronous) pathway.

The computed barrier from separated reactants to the triplet aziridination TS ($^3\text{azir-TS}$) is $\Delta G_{\text{az}}^\ddagger = 24$ kcal/mol (Scheme 14). The $^3\text{Azir-TS}$ has spin density of $0.63 e^-$ on Cu, $0.78 e^-$ on N (NTs), $0.33 e^-$ on C_α , and $-0.10 e^-$ on C_β . The corresponding singlet TS is 12 kcal/mol higher in free energy. This barrier was also calculated with the BP86 functional (reactants and TS geometries fully reoptimized), producing $\Delta G_{\text{az}}^\ddagger = 25$ kcal/mol with that functional.

Going from the aziridination TS to an “open” triplet intermediate (Figure 13B) was exergonic by 22 kcal/mol (18 kcal/mol by virtue of BP86 modeling of this step). The “open” triplet intermediate has an electron spin density of $0.68 e^-$ on Cu, $0.17 e^-$ on the NTs nitrogen, and $0.76 e^-$ on C_α . Thus, the spin density on the benzylic carbon atom has increased significantly vs that of the triplet aziridination TS.

Going from the “open” triplet intermediate (13B) to κ^1 -aziridine product (Figure 13D) is computed to be mildly endergonic, by +8 kcal/mol. C_β – C_α bond rotation was considered for the open triplet intermediate given the stereochemical scrambling seen experimentally (Scheme 5). Constrained optimizations (the H– C_β – C_α –C1 dihedral was

Scheme 13

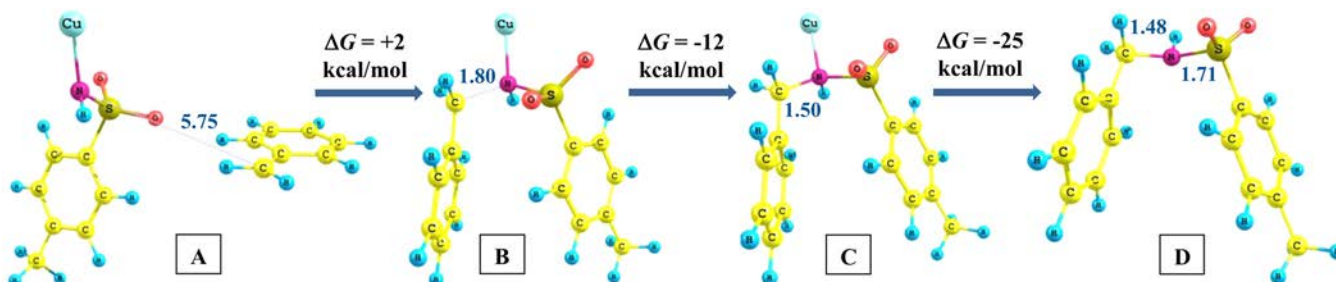
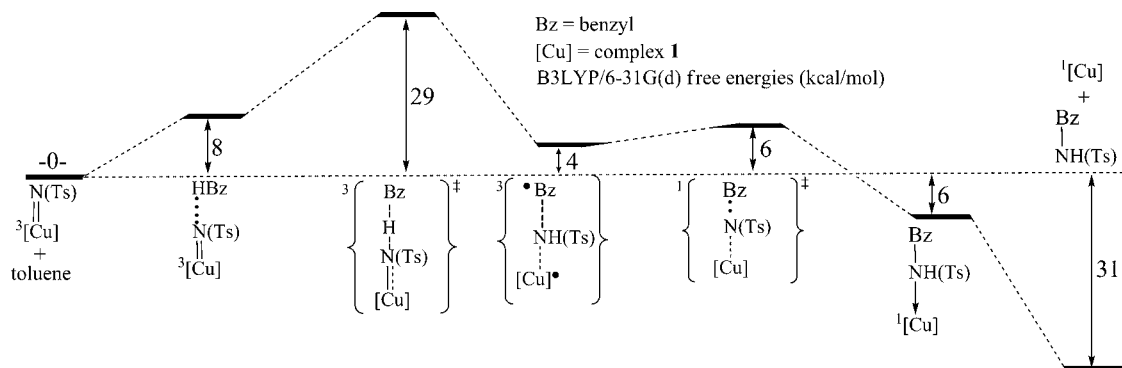


Figure 12. B3LYP/6-31G(d)-computed $^3\{[\text{Cu}]-\text{NHTs}\cdots\text{CH}_2\text{Ph}\}$ caged adduct (A). Singlet radical rebound $\text{TS}_{(\text{Constrained})}$ for the amination of toluene (B) by **1**. Radical rebound product (C). Dissociated product (D). Tripodal ligand was removed from A–C for ease of viewing.

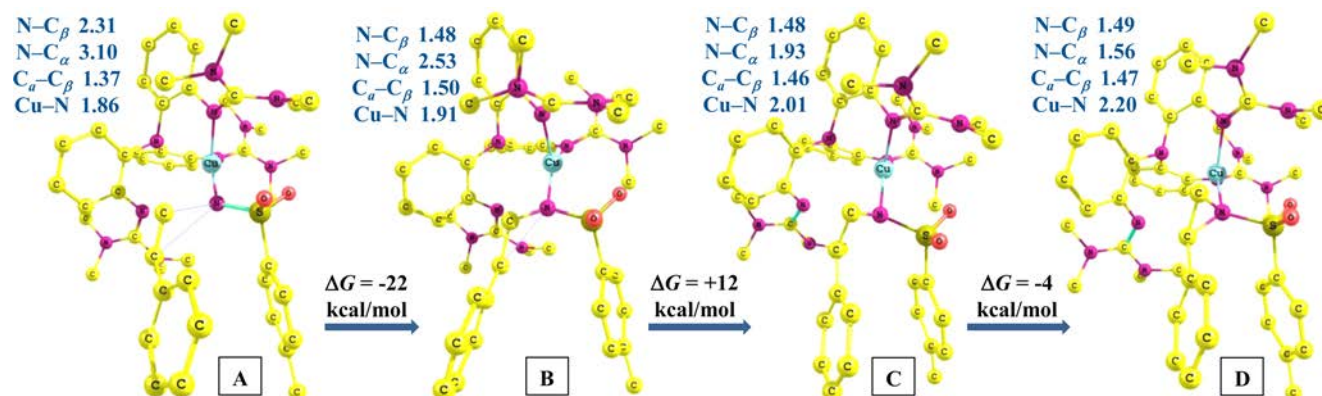
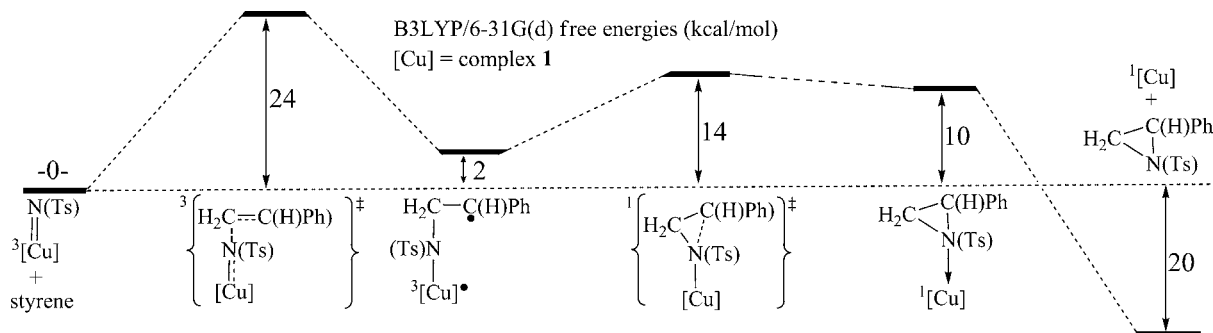


Figure 13. B3LYP/6-31G(d)-computed triplet TS for the aziridination of styrene (A) by **1**. “Open” triplet intermediate (B). Radical rebound TS (C). Singlet aziridine complex (D). Hydrogens are omitted from the figure for ease of viewing.

Scheme 14



fixed to $\pm 90^\circ$) yielded a free energy for rotation around the $\text{C}_\alpha\text{-C}_\beta$ bond of 4 kcal/mol. A radical rebound TS (Figure 13, B \rightarrow C) has $\Delta G^\ddagger = 12$ kcal/mol. These data thus imply potential

rotation about the $\text{C}_\alpha\text{-C}_\beta$ bond of the open triplet intermediate, which is consistent with experimental observations.

The overall formation of aziridine, $^3[\text{Cu}]\text{NTs} + \text{styrene} \rightarrow \text{aziridine} + ^1[\text{Cu}^I]$, is exergonic, with $\Delta G = -20$ kcal/mol. As with the results for toluene amination, this suggests that dissociation of the nitrene-inserted product is facile. Interestingly, the C–N bond lengths in the κ^1 -aziridine product (Figure 13D) are inequivalent, $C_\beta\text{--N}_{\text{TS}} = 1.49$ Å, $C_\alpha\text{--N}_{\text{TS}} = 1.56$ Å. The computed C–N bond lengths in the isolated aziridine product (Figure S36, SI) are $C_\beta\text{--N}_{\text{TS}} = 1.47$ Å, $C_\alpha\text{--N}_{\text{TS}} = 1.50$ Å, and the experimental values (from single-crystal X-ray analysis) are 1.474(4) and 1.492(4) Å, respectively.

For comparative purposes, aziridination transition state geometries (catalyst model 1) were obtained from the parent styrene TS by introducing an electron-donating (MeO) and an electron-withdrawing (CF_3) para-substituent and then initiating a new TS search. As for the unsubstituted olefin substrate discussed above, singlet TS's are higher in energy than triplets for the *p*- CF_3 and *p*-OMe derivatives. The barriers for the initial C–N bond formation ($^3[\text{Cu}]=\text{NTs} + p\text{-Y-C}_6\text{H}_4\text{CH}=\text{CH}_2 \rightarrow ^3\text{Az}^\ddagger$) were calculated to be $\Delta G^\ddagger = 24, 22,$ and 28 kcal/mol for $\text{Y} = \text{H}, \text{OMe},$ and CF_3 , respectively, in accordance with the electrophilic nature of the reaction. The overall formation of the aziridine product had $\Delta G = -20$ kcal/mol for all three substituents modeled ($^3[\text{Cu}]=\text{NTs} + p\text{-Y-C}_6\text{H}_4\text{CH}=\text{CH}_2 \rightarrow ^1[\text{Cu}] + \text{aziridine}$).

Aziridination TS geometries (initial C–N bond formation) for *p*- $\text{Y-C}_6\text{H}_4\text{CH}=\text{CH}_2$ ($\text{Y} = \text{H}, \text{MeO}, \text{CF}_3$) by catalyst model 1 are shown in Table 6. Electron-donating *p*- OCH_3 , associated

Table 6. Transition State (triplet) N–C and C–C (olefin) Bond Lengths for the Aziridination (NTs) of Para-Substituted Styrenes

<i>p</i> -Y	N– C_β	N– C_α	C_α – C_β
H	2.312	3.101	1.371
OCH_3	2.351	3.163	1.370
CF_3	2.268	3.029	1.373

with the lowest C–N bond formation barrier, lengthened the N– C_β and N– C_α bond distances by ~ 0.05 Å vs unsubstituted styrene. For the *p*- CF_3 substituent, N– C_α and N– C_β were similarly shortened. The modest changes in the aziridination TS geometry with the introduction of para-substituents, along with the reasonable computed barriers for torsion about the C_α – C_β bond (see above), are consistent with the experimental observation of the loss of stereochemistry in the aziridination of *trans*-*p*- $\text{Y-C}_6\text{H}_4\text{CH}=\text{CHD}$ (Scheme 5) that does not change much with the para-substituent.

III. CONCLUDING REMARKS

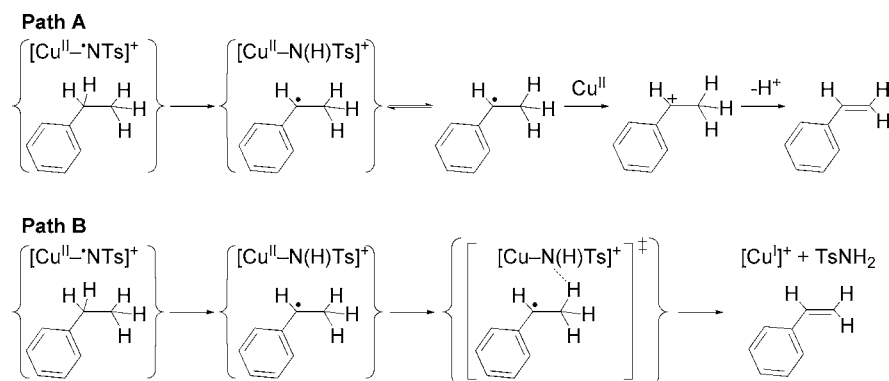
A new C_3 -symmetric Cu^I reagent was studied as a mediator of nitrene-transfer chemistry between donor imidoiodinanes and acceptor C–H- and C=C-containing substrates. Amination of unfunctionalized hydrocarbons is observed at tertiary and secondary, but not primary, C–H sites. Benzylic and α -heteroatom functionalized C–H bonds are also aminated with ease. The substrate range employed and the product yields obtained are competitive with those reported for Rh and Ru reagents or via first-row transition-metal reagents, frequently supported by porphyrinoid ligands. Notably, in addition to the usual amination products, several *tert*-C–H sites are undergoing insertion of nitrile in reactions conducted in MeCN or PhCN, to afford the synthetically useful amidinate framework. Moreover, aziridinations of both electron-poor and electron-

rich olefins are efficiently executed by the Cu^I reagent and are primarily of mechanistic value in our investigations, since several celebrated copper sites are known to mediate the reaction.

The product profiles obtained offer initial mechanistic hints that differentiate copper-mediated nitrene-transfer chemistry from that of rhodium. For instance, products of desaturation are observed with several benzylic and *tert*-C–H substrates, albeit in low yields. Loss of stereochemistry is obtained in C–H nitrene insertions and aziridinations of *cis*-substituted substrates, aziridinations are preferred over C–H allylic insertions, and on average, reactivity is higher with copper at the expense of selectivity. These initial observations point toward the involvement of carboradicals and/or carbocations as distinct intermediates in the insertion/addition of copper–nitrenoids into C–H and C=C bonds.

The presence of carboradicals as the predominant species generated by H atom abstraction in aminations/amidinations and nitrene-addition (initial N–C bond formation) in aziridinations is further substantiated by a series of mechanistic devices. Hammett plots produce linear free energy correlations that require the inclusion of spin-delocalization substituent constants to obtain reasonable fits when both spin and polar effects are significant (aziridination of styrene). When polar effects dominate, as in the case of C–H bond cleavage in toluene aminations, the extracted ρ parameters are very similar to those reported for the well-established radical C–H activation in photolytic toluene brominations. It is also unlikely that hydride-transfer is a dominant path in toluene amination ($\text{Bz-H} + \text{E}^+ \rightarrow \text{Bz}^+ + \text{H-E}$), since the substituent effect on the amination rates for para-substituted toluenes versus toluene is expected to be significantly larger than that observed (for instance, $\rho^+ = -5$ in a well-documented case of hydride-transfer from toluene⁶³). The sizable KIE values are consistent with hydrogen-atom transfer (HAT) involvement, leading to carboradical formation, and are less suited for proton-coupled electron-transfer (PCET)⁶⁴ contributions.⁶⁵ However, PCET paths cannot be excluded, especially for alkyl aromatic and heteroatom-substituted substrates in Table 1 with modest ionization potentials. With respect to aziridination reactions, stepwise addition of nitrene to styrenes is substantiated by secondary KIE values, giving rise to an electron-deficient benzylic site that is better accommodated by a carboradical rather than a carbocation, as suggested by the competitive stereocontrol experiments (Scheme 5) of para-substituted styrenes vs styrene. There is no evidence to suggest that alkyl-substituted olefins switch to a concerted mechanism, since scrambling of stereochemistry is observed, even to a small extent, in all cases examined (Tables 3 and 4). Rather, a gradual increase of the electron-rich character of the substrate radical results in a progressive decrease of the radical recombination barrier, hypothetically approaching a barrierless limit (concerted mechanism) for only exceptionally electron-rich radicals. Finally, radical trap (CBrCl_3) experiments confirm that carboradicals, both solvent-caged and diffusively free, are primary intermediates in C–H aminations, while radical clock studies suggest that solvent-caged radical lifetimes lie in the nanosecond regime, thus providing a sufficient window for competitive rearrangement, stereochemical scrambling, and/or out-of-cage diffusion. Notably, cage effects may play a role in the interpretation of competition kinetics that involve fast, albeit not superfast, radical clocks.

Scheme 15



The participation of carbocationic sites is evident in the product profile of catalytic aminations and can be explained as the outcome of oxidation of diffusively free carboradicals, most likely by Cu^{II} sites. Illustrious precedents of one-electron oxidation of radicals by metal ions abound in the work of Kharasch and Fono⁶⁶ and Kochi and co-workers.^{34,67} Direct evidence of carbocationic involvement is noted in the formation of amidines (Scheme 6) when the catalytic reactions operate in nitriles (MeCN, PhCN). The range of substrates engaged in this reaction is however limited to largely *tert*-C–H sites, due, among other reasons, to the low ionization potentials for tertiary carboradicals. For instance, IP_a values for adamantyl (Table 2, entries 1 and 2) and 2-methyl-2-butyl radicals (entries 5, 6) are only 6.21 ± 0.03 and 6.65 ± 0.04 eV, respectively,⁶⁸ vs 7.36 ± 0.02 , 7.15 ± 0.04 , and 7.20 ± 0.02 eV for isopropyl, cyclohexyl, and benzyl radicals, respectively.⁶⁹ Nevertheless, several carboradicals of alkyl aromatic and α -heteroatom-substituted substrates used in this study may also possess low enough oxidation potentials [$E_{1/2}^{\text{ox}} = 0.73$ V (PhC \cdot H $_2$), 0.37 V (PhC \cdot HCH $_3$), 0.16 V (PhC \cdot (CH $_3$) $_2$), 0.35 V (Ph $_2$ C \cdot H), 0.27 V (Ph $_3$ C \cdot), 0.23 V (Ph $_2$ C \cdot CH $_3$), 0.10 V (9,10-dihydroanthracenyl), and -0.35 V (α -THF) vs SCE in MeCN]⁷⁰ to warrant consideration as possible precursors of carbocations. For cutoff purposes, the most oxidizing Cu^{II} species detected (**6**) has a redox potential of 0.13 V vs SCE. However, the corresponding amidinates were hardly observed, since very low amounts were apparent only in the case of ethylbenzene. A competing reaction for several carbocations is proton abstraction from an adjacent carbon atom, leading to desaturation products (Scheme 15, path A).^{30,71} The reaction is particularly favored for alkyl aromatics, since it furnishes products stabilized by conjugation. Indeed, these products are observed for several substrates in low yields (Table 1, entries 7, 9, 12, and 14) and point toward a precursor carbocationic species, resulting from oxidation of diffusively free carboradicals. However, products of desaturation can also be generated in competition with radical rebound (amination product), via double H atom abstraction by metal-centered moieties⁷² (Scheme 15, path B). The second H atom abstraction can be viewed as a radical disproportionation reaction, competing with radical recombination (affording the amination product). Interestingly, α -arylalkyl radicals tend to favor self-recombination versus disproportionation ($k_r/k_d = 10.2$ for 1-ethylbenzyl radicals in MeCN, as opposed to 0.38 for *tert*-butyl radicals),⁷³ which may explain the low levels of desaturation products for alkyl aromatics according to path B. Alternatively, the low yields may be due to limited out-of-cage diffusion and/or unfavorable oxidation

potentials of substrate radicals according to path A. In the absence of more diagnostic kinetic data that can also evaluate cage effects, the exact provenance of the desaturation products remains uncertain at the present time.

The elusive metal–nitrene moiety ($[\text{Cu}=\text{NTs}]^+$) has not been unequivocally established in the present work but presents a reasonably active entity that seems to be captured in action during insertion of NTs into a ligand-centered NCH $_3$ moiety. Furthermore, the reactivity profile of the corresponding amido species $[\text{Cu}-\text{N}(\text{H})\text{Ts}]^+$ has not yet been elucidated. The ligand vulnerability does not seem to have any effect on catalytic aziridinations, for which the ease of reaction and the excess of olefin used may dictate the product outcome. However, it might interfere with the more challenging amination reactions, although it may also represent a minor component leading to a dead-end path. Nevertheless, experimental and/or computational evidence suggests that the Cu^{I} reagent that possesses one NTs-inserted arm ($-\text{NCH}_2\text{NHTs}$ in lieu of $-\text{NMe}$) and even a demethylated congener ($-\text{NH}$ in lieu of $-\text{NMe}$) have the potential to be active precatalysts. Other ligand-centered, redox-related events cannot be excluded at the present time, but transformations such as those encountered with the much more electron-rich triphenylamido-amine ligands (one-electron oxidation followed by ligand rearrangement)^{25b,74} have not been observed.

Resolving these challenges with respect to the reactivity and selectivity of individual metal–nitrene moieties, along with an expansion toward more difficult to aminate primary C–H bonds, will be the focus of future investigations.

■ ASSOCIATED CONTENT

📄 Supporting Information

Experimental procedures, analytical data for all compounds, computational details, and CIF files. This material is available free of charge via the Internet at <http://pubs.acs.org>.

■ AUTHOR INFORMATION

Corresponding Authors

Lee.Cronin@glasgow.ac.uk;
t@unt.edu;
pericles@mst.edu

Notes

The authors declare no competing financial interest.

■ ACKNOWLEDGMENTS

We gratefully acknowledge the NSF for partial support of this research through grants CHE-0412959 (P.S.) and CHE-

1057785 (T.R.C. and D.P.); the EPSRC grants EP/H024107/1, EP/I033459/1, EP/J015156/1; the Royal-Society Wolfson Foundation for a Merit Award; and the University of Glasgow (L.C.); and the Special Account of Research Grants of the University of Athens (P.P.). We thank Drs. Richard Dawes, Lia Sotiriou-Leventis, Shubhen Kapila, Rex Gerald, II, Sudip Mohapatra, Wei Wycoff, Nathan Leigh, and Ms. Ming Huang for valuable experimental assistance and fruitful discussions. We are also indebted to Prof. Steve Davies and Dr. J. E. Thompson (University of Oxford, UK), Dr. Regine Herbst-Irmer and Dr. George M. Sheldrick (University of Göttingen, Germany), and Prof. Konstantinos Methenitis (University of Athens, Greece) for useful advice.

REFERENCES

- (1) Taube, H. In *Mechanistic Aspects of Inorganic Reactions*; ACS Symposium Series 198; Rorabacher, D. B., Endicott, J. F., Eds.; American Chemical Society: Washington, DC, 1982; Chapter 7, pp 151–179.
- (2) Mayer, J. M. *Acc. Chem. Res.* **2011**, *44*, 36–46.
- (3) (a) Atienza, C. C. H.; Bowman, A. C.; Lobkovsky, E.; Chirik, P. J. *J. Am. Chem. Soc.* **2010**, *132*, 16343–16345. (b) Berry, J. F.; Bill, E.; Bothe, E.; DeBeer George, S.; Mienert, B.; Neese, F.; Wieghardt, K. *Science* **2006**, *312*, 1937–1941. (c) DuBois, J.; Tomooka, C. S.; Hong, J.; Carreira, E. M. *Acc. Chem. Res.* **1997**, *30*, 364–372. (d) Scepaniak, J. J.; Vogel, C. S.; Khusniyarov, M. M.; Heinemann, F. W.; Meyer, K.; Smith, J. M. *Science* **2011**, *331*, 1049–1052. (e) Betley, T. A.; Peters, J. C. *J. Am. Chem. Soc.* **2004**, *126*, 6252–6254. (f) Curley, J. J.; Cook, T. R.; Reece, S. Y.; Müller, P.; Cummins, C. C. *J. Am. Chem. Soc.* **2008**, *130*, 9394–9405. (g) Vogel, C.; Heinemann, F. W.; Sutter, J.; Anthon, C.; Meyer, K. *Angew. Chem., Int. Ed.* **2008**, *47*, 2681–2684.
- (4) (a) Holm, R. H. *Chem. Rev.* **1987**, *87*, 1401–1449. (b) Murray, L. J.; Lippard, S. J. *Acc. Chem. Res.* **2007**, *40*, 466–474. (c) Cooper, H. L. R.; Mishra, G.; Huang, X.; Pender-Cudlip, M.; Austin, R. N.; Shanklin, J.; Groves, J. T. *J. Am. Chem. Soc.* **2012**, *134*, 20365–20375. (d) Que, L., Jr.; Tolman, W. B. *Nature* **2008**, *455*, 333–340. (e) McDonald, A. R.; Que, L., Jr. *Coord. Chem. Rev.* **2013**, *257*, 414–428. (f) Chen, M. S.; White, M. C. *Science* **2010**, *327*, 566–571. (g) Nam, W.; Lee, Y.-M.; Fukuzumi, S. *Acc. Chem. Res.* **2014**, *47*, 1146–1154. (h) Abu-Omar, M. M. In *Physical Inorganic Chemistry, Reactions, Processes, and Applications*; Bakac, A., Ed.; John Wiley & Sons, Inc.: Hoboken, NJ, 2010; pp 75–108. (i) Peterson, R. L.; Himes, R. A.; Kotani, H.; Suenobu, T.; Tian, L.; Siegler, M.; Solomon, E. I.; Fukuzumi, S.; Karlin, K. D. *J. Am. Chem. Soc.* **2011**, *133*, 1702–1705. (j) Kundu, S.; Thompson, J. V. K.; Ryabov, A. D.; Collins, T. J. *J. Am. Chem. Soc.* **2011**, *133*, 18546–18549. (k) Taguchi, T.; Gupta, R.; Lassalle-Kaiser, B.; Boyce, D. W.; Yachandra, V. K.; Tolman, W. B.; Yano, J.; Hendrich, M. P.; Borovik, A. S. *J. Am. Chem. Soc.* **2012**, *134*, 1996–1999.
- (5) (a) Donahue, J. P. *Chem. Rev.* **2006**, *106*, 4747–4783. (b) Yang, L.; Tehrani, J.; Tolman, W. B. *Inorg. Chem.* **2011**, *50*, 2606–2612. (c) Wang, J.-J.; Kryatova, O. P.; Rybak-Akimova, E. V.; Holm, R. H. *Inorg. Chem.* **2004**, *43*, 8092–8101.
- (6) (a) Matyjaszewski, K. *Macromolecules* **2012**, *45*, 4015–4039. (b) Pintauer, T.; Matyjaszewski, K. *Chem. Soc. Rev.* **2008**, *37*, 1087–1097. (c) Ouchi, M.; Terashima, T.; Sawamoto, M. *Chem. Rev.* **2009**, *109*, 4963–5050.
- (7) (a) Hartwig, J. F. *Acc. Chem. Res.* **2012**, *45*, 864–873. (b) Mkhallid, I. A. I.; Barnard, J. H.; Marder, T. B.; Murphy, J. M.; Hartwig, J. F. *Chem. Rev.* **2010**, *110*, 890–931. (c) Obligacion, J. V.; Semproni, S. P.; Chirik, P. J. *J. Am. Chem. Soc.* **2014**, *136*, 4133–4136.
- (8) (a) Doyle, M. P.; Forbes, D. C. *Chem. Rev.* **1998**, *98*, 911–935. (b) Davies, H. M. L.; Beckwith, R. E. J. *Chem. Rev.* **2003**, *103*, 2861–2903. (c) Davies, H. M. L.; Manning, J. R. *Nature* **2008**, *451*, 417–424.
- (9) (a) Zalatan, D. N.; Du Bois, J. *Top. Curr. Chem.* **2010**, *292*, 347–378. (b) Roizen, J. L.; Harvey, M. E.; Du Bois, J. *Acc. Chem. Res.* **2012**, *45*, 911–922. (c) Gephart, R. T., III; Warren, T. H. *Organometallics* **2012**, *31*, 7728–7752. (d) Collet, F.; Lescot, C.; Dauban, P. *Chem. Rev.* **2011**, *40*, 1926–1936. (e) Uchida, T.; Katsuki, T. *Chem. Rev.* **2014**, *14*, 117–129. (f) Pellissier, H. *Tetrahedron* **2010**, *66*, 1509–1555. (g) Díaz-Requejo, M. M.; Pérez, P. J. *Chem. Rev.* **2008**, *108*, 3379–3394. (h) Müller, P.; Fruit, C. *Chem. Rev.* **2003**, *103*, 2905–2919. (10) Bariwal, J.; Van der Eycken, E. *Chem. Soc. Rev.* **2013**, *42*, 9283–9303. (11) (a) Svastits, E. W.; Dawson, J. H.; Breslow, R.; Gellman, S. H. *J. Am. Chem. Soc.* **1985**, *107*, 6427–6428. (b) Matthews, M. L.; Chang, W.-C.; Layne, A. P.; Miles, L. A.; Krebs, C.; Bollinger, J. M., Jr. *Nat. Chem. Biol.* **2014**, *10*, 209–215. (c) McIntosh, J. A.; Coelho, P. S.; Farwell, C. C.; Wang, Z. J.; Lewis, J. C.; Brown, T. R.; Arnold, F. H. *Angew. Chem., Int. Ed.* **2013**, *52*, 9309–9312. (d) Singh, R.; Bordeaux, M.; Fasan, R. *ACS Catal.* **2014**, *4*, 546–552. (e) Mahy, J.-P.; Ciesielski, J.; Dauban, P. *Angew. Chem., Int. Ed.* **2014**, *53*, 6862–6864. (12) (a) Aguila, M. J. B.; Badiei, Y. M.; Warren, T. H. *J. Am. Chem. Soc.* **2013**, *135*, 9399–9406. (b) Badiei, Y. M.; Dinescu, A.; Dai, X.; Palomino, R. M.; Heinemann, F. W.; Cundari, T. R.; Warren, T. H. *Angew. Chem., Int. Ed.* **2008**, *47*, 9961–9964. (c) Barman, D. N.; Liu, P.; Houk, K. N.; Nicholas, K. M. *Organometallics* **2010**, *29*, 3404–3412. (d) Barman, D.; Nicholas, K. M. *Tetrahedron Lett.* **2010**, *51*, 1815–1818. (e) Fructos, M. R.; Trofimenko, S.; Díaz-Requejo, M. M.; Pérez, P. J. *J. Am. Chem. Soc.* **2006**, *128*, 11784–11791. (f) Gómez-Emeterio, B. P.; Urbano, J.; Díaz-Requejo, M. M.; Pérez, P. J. *Organometallics* **2008**, *27*, 4126–4130. (g) Díaz-Requejo, M. M.; Pérez, P. J.; Brookhart, M.; Templeton, J. L. *Organometallics* **1997**, *16*, 4399–4402. (h) Lebel, H.; Parmentier, M. *Pure Appl. Chem.* **2010**, *82*, 1827–1833. (i) Lebel, H.; Lectard, S.; Parmentier, M. *Org. Lett.* **2007**, *9*, 4797–4800. (j) Powell, D. A.; Fan, H. *J. Org. Chem.* **2010**, *75*, 2726–2729. (k) Pelletier, G.; Powell, D. A. *Org. Lett.* **2006**, *8*, 6031–6034. (l) Li, Z.; Capretto, D. A.; Rahaman, R.; He, C. *Angew. Chem., Int. Ed.* **2007**, *46*, 5184–5186. (m) Li, Z.; Ding, X.; He, C. *J. Org. Chem.* **2006**, *71*, 5876–5880. (n) Rigoli, J. W.; Weatherly, C. D.; Alderson, J. M.; Vo, B. T.; Schomaker, J. M. *J. Am. Chem. Soc.* **2013**, *135*, 17238–17241. (o) Comba, P.; Haaf, C.; Lienke, A.; Muruganatham, A.; Wade, P. H. *Chem.—Eur. J.* **2009**, *15*, 10880–10887. (p) Vedernikov, A. N.; Caulton, K. G. *Chem. Commun.* **2004**, 162–163. (q) Evans, D. A.; Faul, M. M.; Bilodeau, M. T. *J. Am. Chem. Soc.* **1994**, *116*, 2742–2753. (r) Li, Z.; Quan, R. W.; Jacobsen, E. N. *J. Am. Chem. Soc.* **1995**, *117*, 5889–5890. (s) Dash, C.; Yousufuddin, M.; Cundari, T. R.; Dias, H. V. R. *J. Am. Chem. Soc.* **2013**, *135*, 15479–15488. (13) (a) Fiori, K. W.; Du Bois, J. *J. Am. Chem. Soc.* **2007**, *129*, 562–568. (b) Zalatan, D. N.; Du Bois, J. *J. Am. Chem. Soc.* **2009**, *131*, 7558–7559. (c) Fiori, K. W.; Espino, C. G.; Brodsky, B. H.; Du Bois, J. *Tetrahedron* **2009**, *65*, 3042–3051. (d) Liang, C.; Collet, F.; Robert-Peillard, F.; Müller, P.; Dodd, R. H.; Dauban, P. *J. Am. Chem. Soc.* **2008**, *130*, 343–350. (e) Liang, C.; Robert-Peillard, F.; Fruit, C.; Müller, P.; Dodd, R. H.; Dauban, P. *Angew. Chem., Int. Ed.* **2006**, *45*, 4641–4644. (f) Nägeli, I.; Baud, C.; Bernardinelli, G.; Jacquier, Y.; Moran, M.; Müller, P. *Helv. Chim. Acta* **1997**, *80*, 1087–1105. (g) Huard, K.; Lebel, H. *Chem.—Eur. J.* **2008**, *14*, 6222–6230. (h) Lebel, H.; Huard, K.; Lectard, S. *J. Am. Chem. Soc.* **2005**, *127*, 14198–14199. (i) Reddy, R. P.; Davies, H. M. L. *Org. Lett.* **2006**, *8*, 5013–5016. (j) Nguyen, Q.; Sun, K.; Driver, T. G. *J. Am. Chem. Soc.* **2012**, *134*, 7262–7265. (k) Jat, J. L.; Paudyal, M. P.; Gao, H.; Xu, Q.-L.; Yousufuddin, M.; Devarajan, D.; Ess, D. H.; Kürti, L.; Falck, J. R. *Science* **2014**, *343*, 61–65. (14) (a) King, E. R.; Hennessy, E. T.; Betley, T. A. *J. Am. Chem. Soc.* **2011**, *133*, 4917–4923. (b) Paradine, S. M.; White, M. C. *J. Am. Chem. Soc.* **2012**, *134*, 2036–2039. (c) Cowley, R. E.; Eckert, N. A.; Vaddadi, S.; Figg, T. M.; Cundari, T. R.; Holland, P. L. *J. Am. Chem. Soc.* **2011**, *133*, 9796–9811. (d) Nguyen, Q.; Nguyen, T.; Driver, T. G. *J. Am. Chem. Soc.* **2013**, *135*, 620–623. (e) Wang, J.; Frings, M.; Bolm, C. *Angew. Chem., Int. Ed.* **2013**, *52*, 8661–8665. (f) Liu, Y.; Guan, X.; Wong, E. L.-M.; Liu, P.; Huang, J.-S.; Che, C.-M. *J. Am. Chem. Soc.* **2013**, *135*, 7194–7204. (g) Liu, Y.; Che, C. M. *Chem.—Eur. J.* **2010**, *16*, 10494–10501. (h) Mankad, N. P.; Müller, P.; Peters, J. C. *J. Am. Chem. Soc.* **2010**, *132*, 4083–4085. (i) Jensen, M. P.; Mehn, M. P.; Que, L., Jr. *Angew. Chem., Int. Ed.* **2003**, *42*, 4357–4360. (j) Srivastava,

- R. S.; Nicholas, K. M. *J. Am. Chem. Soc.* **1997**, *119*, 3302–3310.
- (k) Breslow, R.; Gellman, S. H. *J. Am. Chem. Soc.* **1983**, *105*, 6728–6729.
- (l) Mansuy, D.; Mahy, J.-P.; Dureault, A.; Bedi, G.; Battioni, P. *J. Chem. Soc., Chem. Commun.* **1984**, 1161–1163.
- (m) Mahy, J.-P.; Bedi, G.; Battioni, P.; Mansuy, D. *New J. Chem.* **1989**, *13*, 651–657.
- (15) (a) Lu, H.; Jiang, H.; Wojtas, L.; Zhang, X. P. *Angew. Chem., Int. Ed.* **2010**, *49*, 10192–10196. (b) Lu, H.; Tao, J.; Jones, J. E.; Wojtas, L.; Zhang, X. P. *Org. Lett.* **2010**, *12*, 1248–1251. (c) Lu, H.; Subbarayan, V.; Tao, J.; Zhang, X. P. *Organometallics* **2010**, *29*, 389–393. (d) Lyaskovskyy, V.; Suarez, A. I. O.; Lu, H.; Jiang, H.; Zhang, X. P.; de Bruin, B. *J. Am. Chem. Soc.* **2011**, *133*, 12264–12273. (e) Suarez, A. I. O.; Jiang, H.; Zhang, X. P.; de Bruin, B. *Dalton Trans.* **2011**, *40*, 5697–5705. (f) Caselli, A.; Gallo, E.; Fantauzzi, S.; Morlacchi, S.; Ragaini, F.; Cenini, S. *Eur. J. Inorg. Chem.* **2008**, 3009–3019. (g) Ragaini, F.; Penoni, A.; Gallo, E.; Tollari, S.; Gotti, C. L.; Lapadula, M.; Mangioni, E.; Cenini, S. *Chem.—Eur. J.* **2003**, *9*, 249–259. (h) King, E. R.; Hennessy, E. T.; Betley, T. *J. Am. Chem. Soc.* **2011**, *133*, 4917–4923. (i) Shay, D. T.; Yap, G. P. A.; Zakharov, L. N.; Rheingold, A. L.; Theopold, K. H. *Angew. Chem., Int. Ed.* **2005**, *44*, 1508–1510. (j) Ichinose, M.; Suematsu, H.; Yasutomi, Y.; Nishioka, Y.; Uchida, T.; Katsuki, T. *Angew. Chem., Int. Ed.* **2011**, *50*, 9884–9887. (k) Kang, T.; Kim, Y.; Lee, D.; Wang, Z.; Chang, S. *J. Am. Chem. Soc.* **2014**, *136*, 4141–4144.
- (16) (a) Wiese, S.; McAfee, J. L.; Pahls, D. R.; McMullin, C. L.; Cundari, T. R.; Warren, T. H. *J. Am. Chem. Soc.* **2012**, *134*, 10114–10121. (b) Kogut, E.; Wiencko, H. L.; Zhang, L.; Cordeau, D. E.; Warren, T. H. *J. Am. Chem. Soc.* **2005**, *127*, 11248–11249. (c) Laskowski, C. A.; Miller, A. J. M.; Hillhouse, G. L.; Cundari, T. R. *J. Am. Chem. Soc.* **2011**, *133*, 771–773. (d) Iluc, V. M.; Miller, A. J. M.; Anderson, J. S.; Monreal, M. J.; Mehn, M. P.; Hillhouse, G. L. *J. Am. Chem. Soc.* **2011**, *133*, 13055–13063. (e) Harrold, N. D.; Waterman, R.; Hillhouse, G. L.; Cundari, T. R. *J. Am. Chem. Soc.* **2009**, *131*, 12872–12873.
- (17) (a) Harvey, M. E.; Musaev, D.; Du Bois, J. *J. Am. Chem. Soc.* **2011**, *133*, 17207–17216. (b) Leung, S. K.-Y.; Tsui, W.-M.; Huang, J.-S.; Che, C.-M.; Liang, J.-L.; Zhu, N. *J. Am. Chem. Soc.* **2005**, *127*, 16629–16640. (c) Liang, J.-L.; Huang, J.-S.; Yu, X.-Q.; Zhu, N.; Che, C.-M. *Chem.—Eur. J.* **2002**, *8*, 1563–1572. (d) Au, S.-M.; Huang, J.-S.; Yu, W.-Y.; Fung, W.-H.; Che, C.-M. *J. Am. Chem. Soc.* **1999**, *121*, 9120–9132. (e) Xiao, W.; Wei, J.; Zhou, C.-Y.; Che, C.-M. *Chem. Commun.* **2013**, *49*, 4619–4621. (f) Zdilla, M. J.; Dexheimer, J. L.; Abu-Omar, M. M. *J. Am. Chem. Soc.* **2007**, *129*, 11505–11511. (g) Nishioka, Y.; Uchida, T.; Katsuki, T. *Angew. Chem., Int. Ed.* **2013**, *52*, 1739–1742. (h) Kohmura, Y.; Katsuki, T. *Tetrahedron Lett.* **2001**, *42*, 3339–3342.
- (18) (a) Lu, H.; Zhang, X. P. *Chem. Soc. Rev.* **2011**, *40*, 1899–1909. (b) Ruppel, J. V.; Fields, K. B.; Snyder, N. L.; Zhang, X. P. In *Handbook of Porphyrin Science*; Eds. Kadish, K. M., Smith, K. M., Guillard, R., Eds.; World Scientific: Singapore, 2010; Vol. 10, Chapter 43, pp 1–182.
- (19) (a) Tekarli, S. M.; Williams, T. G.; Cundari, T. R. *J. Chem. Theory Comput.* **2009**, *5*, 2959–2966. (b) Cundari, T. R.; Dinescu, A.; Kazi, A. B. *Inorg. Chem.* **2008**, *47*, 10067–10072. (c) Moreau, Y.; Chen, H.; Derat, E.; Hirao, H.; Bolm, C.; Shaik, S. *J. Phys. Chem. B* **2007**, *111*, 10288–10299.
- (20) Maestre, L.; Sameira, W. M. C.; Díaz-Requejo, M. M.; Maseras, F.; Pérez, P. *J. Am. Chem. Soc.* **2013**, *135*, 1338–1348.
- (21) (a) Kundu, S.; Miceli, E.; Farquhar, E.; Pfaff, F. F.; Kuhlmann, U.; Hildebrandt, P.; Braun, B.; Greco, C.; Ray, K. *J. Am. Chem. Soc.* **2012**, *134*, 14710–14713. (b) Dielmann, F.; Andrada, D. M.; Frenking, G.; Bertrand, G. *J. Am. Chem. Soc.* **2014**, *136*, 3800–3802.
- (22) (a) Li, Z.; Conser, K. R.; Jacobsen, E. N. *J. Am. Chem. Soc.* **1993**, *115*, 5326–5327. (b) Evans, D. A.; Faul, M. M.; Bildeau, M. T.; Anderson, B. A.; Barnes, D. M. *J. Am. Chem. Soc.* **1993**, *115*, 5328–5329.
- (23) (a) Desimoni, G.; Faita, G.; Jørgensen, K. A. *Chem. Rev.* **2006**, *106*, 3561–3651. (b) Yoon, T. P.; Jacobsen, E. N. *Science* **2003**, *299*, 1691–1693.
- (24) (a) Peterson, R. L.; Ginsbach, J. W.; Cowley, R. E.; Qayyum, M. F.; Himes, R. A.; Siegler, M. A.; Moore, C. D.; Hedman, B.; Hodgson, K. O.; Fukuzumi, S.; Solomon, E. I.; Karlin, K. D. *J. Am. Chem. Soc.* **2013**, *135*, 16454–16467. (b) England, J.; Guo, Y.; Farquhar, E. R.; Young, V. G., Jr.; Münck, E.; Que, L., Jr. *J. Am. Chem. Soc.* **2010**, *132*, 8635–8644. (c) Pfaff, F. F.; Kundu, S.; Risch, M.; Pandian, S.; Heims, F.; Pryjomska-Ray, I.; Haack, P.; Metzinger, R.; Bill, E.; Dau, H.; Comba, P.; Ray, K. *Angew. Chem., Int. Ed.* **2011**, *50*, 1711–1715. (d) Lanci, M. P.; Smirnov, V. V.; Cramer, C. J.; Gauchenova, E. V.; Sundermeyer, J.; Roth, J. P. *J. Am. Chem. Soc.* **2007**, *129*, 14697–14709.
- (25) (a) Jones, M. B.; MacBeth, C. E. *Inorg. Chem.* **2007**, *46*, 8117–8119. (b) Çelenligil-Çetin, R.; Paraskevopoulou, P.; Dinda, R.; Staples, R. J.; Sinn, E.; Rath, N. P.; Stavropoulos, P. *Inorg. Chem.* **2008**, *47*, 1165–1172.
- (26) Göbel, M.; Klapötke, T. M. *Chem. Commun.* **2007**, 3180–3182.
- (27) Raab, V.; Kipke, J.; Burghaus, O.; Sundermeyer, J. *Inorg. Chem.* **2001**, *40*, 6964–6971.
- (28) A similar resolution of four methyl peaks ($\delta = 3.19, 2.70, 2.64, 2.58$ ppm), albeit at 25 °C in CD₃CN, has been noted for [Cu^I(TMG₃tren)](ClO₄). See ref 27.
- (29) (a) Corey, E. J.; Posner, G. H.; Atkinson, R. F.; Wingard, A. K.; Halloran, D. J.; Radzik, D. M.; Nash, J. J. *J. Org. Chem.* **1989**, *54*, 389–393. (b) Cristol, S. J.; Barasch, W.; Tieman, C. H. *J. Am. Chem. Soc.* **1955**, *77*, 583–590.
- (30) (a) Buist, P. H. *Nat. Prod. Rep.* **2004**, *21*, 249–262. (b) Buist, P. H.; Behrouzian, B. *J. Am. Chem. Soc.* **1996**, *118*, 6295–6296. (c) Jin, Y.; Lipscomb, J. D. *J. Biol. Inorg. Chem.* **2001**, *6*, 717–725.
- (31) (a) Dowers, T. S.; Rock, D. A.; Rock, D. A.; Jones, J. P. *J. Am. Chem. Soc.* **2004**, *126*, 8868–8869. (b) Li, C.; Wu, W.; Kumar, D.; Shaik, S. *J. Am. Chem. Soc.* **2006**, *128*, 394–395.
- (32) See also ref 12a.
- (33) (a) Ritter, J. J.; Minieri, P. P. *J. Am. Chem. Soc.* **1948**, *70*, 4045–4048. (b) Ritter, J. J.; Kalish, J. *J. Am. Chem. Soc.* **1948**, *70*, 4048–4050.
- (34) Rollick, K. L.; Kochi, J. K. *J. Am. Chem. Soc.* **1982**, *104*, 1319–1330.
- (35) (a) de Lijser, H. J. P.; Arnold, D. R. *J. Phys. Chem. A* **1998**, *102*, 5592–5598. (b) Engel, P. S.; Lee, W.-K.; Marschke, G. E.; Shine, H. J. *J. Org. Chem.* **1987**, *52*, 2813–2817. (c) Bae, D. H.; Engel, P. S.; Hoque, A. K. M. M.; Keys, D. E.; Lee, W.-K.; Shaw, R. W.; Shine, H. J. *J. Am. Chem. Soc.* **1985**, *107*, 2561–2562. (d) Michaudel, Q.; Thevenet, D.; Baran, P. S. *J. Am. Chem. Soc.* **2012**, *134*, 2547–2550.
- (36) Johnson, J. S.; Evans, D. A. *Acc. Chem. Res.* **2000**, *33*, 325–335.
- (37) Bagchi, V.; Paraskevopoulou, P.; Choudhury, A.; Stavropoulos, P. Manuscript in preparation.
- (38) Raab, V. *Peralkyl Guanidines in Copper Catalyzed Oxidative Transformations and Novel Proton Sponges*. Ph.D. Thesis, Philipps-Universität Marburg, 2001, Chapter 3.2, p 7.
- (39) Jiang, X.-K. *Acc. Chem. Res.* **1997**, *30*, 283–289.
- (40) (a) Jiang, X.-K.; Ji, G.-Z. *J. Org. Chem.* **1992**, *57*, 6051–6056. (b) Jiang, X.-K.; Liu, W. W.-Z. *J. Phys. Org. Chem.* **1994**, *7*, 96–104.
- (41) Dingtürk, S.; Jackson, R. A. *J. Chem. Soc., Perkins 2* **1981**, 1127–1131.
- (42) Hennessy, E. T.; Liu, R. Y.; Iovan, D. A.; Duncan, R. A.; Betley, T. A. *Chem. Sci.* **2014**, *5*, 1526–1532.
- (43) Kim, S. S.; Choi, S. Y.; Kang, C. H. *J. Am. Chem. Soc.* **1985**, *107*, 4234–4237.
- (44) Park, S. H.; Kwak, J.; Shin, K.; Ryu, J.; Park, Y.; Chang, S. *J. Am. Chem. Soc.* **2014**, *136*, 2492–2502.
- (45) Sorokin, A.; Robert, A.; Meunier, B. *J. Am. Chem. Soc.* **1993**, *115*, 7293–7299.
- (46) Lamar, A. A.; Nicholas, K. M. *J. Org. Chem.* **2010**, *75*, 7644–7650.
- (47) Poirier, R. A.; Wang, Y.; Westaway, K. C. *J. Am. Chem. Soc.* **1994**, *116*, 2526–2533.
- (48) (a) Ogliaro, F.; Harris, N.; Cohen, S.; Filatov, M.; de Visser, S. P.; Shaik, S. *J. Am. Chem. Soc.* **2000**, *122*, 8977–8989. (b) Shaik, S.; de Visser, S. P.; Ogliaro, F.; Schwarz, H.; Schröder, D. *Curr. Opin. Chem. Biol.* **2002**, *6*, 556–567.

- (49) (a) Garr, C. D.; Finke, R. G. *Inorg. Chem.* **1993**, *32*, 4414–4421. (b) Stickrath, A. B.; Carroll, E. C.; Dai, X.; Harris, D. A.; Rury, A.; Smith, B.; Tang, K.-C.; Wert, J.; Sension, R. J. *J. Phys. Chem. A* **2009**, *113*, 8513–8522.
- (50) (a) Bravo, A.; Bjørsvik, H.-R.; Fontana, F.; Minisci, F.; Serri, A. *J. Org. Chem.* **1996**, *61*, 9409–9416. (b) Recupero, F.; Bravo, A.; Bjørsvik, H.-R.; Fontana, F.; Minisci, F.; Piredda, M. *J. Chem. Soc., Perkin Trans. 2* **1997**, 2399–2405.
- (51) Khusnutdinov, R. I.; Shchadneva, N. A.; Khisamova, L. F.; Mayakova, Y. Y.; Dzhemilev, U. M. *Russ. J. Org. Chem.* **2011**, *47*, 1898–1900.
- (52) Hollis, R.; Hughes, L.; Bowry, V. W.; Ingold, K. U. *J. Org. Chem.* **1992**, *57*, 4284–4287.
- (53) (a) Davis, F. A.; Song, M.; Augustine, A. *J. Org. Chem.* **2006**, *71*, 2779–2786. (b) Selander, N.; Szabó, K. J. *J. Org. Chem.* **2009**, *74*, 5695–5698.
- (54) Yang, H.; Fang, L.; Zhang, M.; Zhu, C. *Eur. J. Org. Chem.* **2009**, 666–672.
- (55) Csatayová, K.; Davies, S. G.; Lee, J. A.; Ling, K. B.; Roberts, P. M.; Russell, A. J.; Thomson, J. E. *Tetrahedron* **2010**, *66*, 8420–8440.
- (56) Our physicochemical data for the ring-closed products differ significantly from those reported (ref 12c).
- (57) Austin, R. N.; Luddy, K.; Erickson, K.; Pender-Cudlip, M.; Bertrand, E.; Deng, D.; Buzdygon, R. S.; van Beilen, J. B.; Groves, J. T. *Angew. Chem., Int. Ed.* **2008**, *47*, 5232–5234.
- (58) Prat, I.; Mathieson, J. S.; Güell, M.; Ribas, X.; Luis, J. M.; Cronin, L.; Costas, M. *Nat. Chem.* **2011**, *3*, 788–793.
- (59) Maiti, D.; Lee, D.-H.; Gaoutchenova, K.; Würtele, C.; Holthausen, M. C.; Narducci Sarjeant, A. A.; Sundermeyer, J.; Schindler, S.; Karlin, K. D. *Angew. Chem., Int. Ed.* **2008**, *47*, 82–85.
- (60) (a) Avenier, F.; Gouré, E.; Dubourdeaux, P.; Sénèque, O.; Oddou, J.-L.; Pécaut, J.; Chardon-Noblat, S.; Deronzier, A.; Latour, J.-M. *Angew. Chem., Int. Ed.* **2008**, *47*, 715–717. (b) King, E. R.; Betley, T. A. *Inorg. Chem.* **2009**, *48*, 2361–2363.
- (61) Cundari, T. R.; Morello, G. R. *J. Org. Chem.* **2009**, *74*, 5711–5714.
- (62) Cundari, T. R.; Russo, M. *J. Chem. Inf. Comput. Sci.* **2001**, *41*, 281–287.
- (63) Larsen, A. S.; Wang, K.; Lockwood, M. A.; Rice, G. L.; Won, T.-J.; Lovell, S.; Sadílek, M.; Tureček, F.; Mayer, J. M. *J. Am. Chem. Soc.* **2002**, *124*, 10112–10123.
- (64) Mayer, J. M.; Larsen, A. S.; Bryant, J. R.; Wang, K.; Lockwood, M.; Rice, G.; Won, T.-J. In *Activation and Functionalization of C–H Bonds*; ACS Symposium Series 885; Goldberg, K. I., Goldman, A. S., Eds.; American Chemical Society: Washington, DC, 2004; Chapter 21, pp 356–369.
- (65) Park, J.; Lee, Y.-M.; Nam, W.; Fukuzumi, S. *J. Am. Chem. Soc.* **2013**, *135*, 5052–5061.
- (66) Kharasch, M. S.; Fono, A. *J. Org. Chem.* **1959**, *24*, 606–614.
- (67) (a) Kochi, J. K.; Mog, D. M. *J. Am. Chem. Soc.* **1965**, *87*, 522–528. (b) Kochi, J. K. *Science* **1967**, *155*, 415–424.
- (68) Kruppa, G. H.; Beauchamp, J. L. *J. Am. Chem. Soc.* **1986**, *108*, 2162–2169.
- (69) (a) Houle, F. A.; Beauchamp, J. L. *J. Am. Chem. Soc.* **1979**, *101*, 4067–4074. (b) Houle, F. A.; Beauchamp, J. L. *J. Phys. Chem.* **1981**, *85*, 3456–3461. (c) Houle, F. A.; Beauchamp, J. L. *J. Am. Chem. Soc.* **1978**, *100*, 3290–3294.
- (70) (a) Wayner, D. D. M.; McPhee, D. J.; Griller, D. *J. Am. Chem. Soc.* **1988**, *110*, 132–137. (b) Griller, D.; Martinho Simões, J. A.; Mulder, P.; Sim, B. A.; Wayner, D. D. M. *J. Am. Chem. Soc.* **1989**, *111*, 7872–7876. (c) Zhang, X.; Bordwell, F. G. *J. Org. Chem.* **1992**, *57*, 4163–4168. (d) Holm, A. H.; Brinck, T.; Daasbjerg, K. *J. Am. Chem. Soc.* **2005**, *127*, 2677–2685.
- (71) Voica, A.-F.; Mendoza, A.; Gutekunst, W. R.; Fraga, J. O.; Baran, P. S. *Nat. Chem.* **2012**, *4*, 629–635.
- (72) (a) Bigi, M. A.; Reed, S. A.; White, M. C. *Nat. Chem.* **2011**, *3*, 216–222. (b) Hull, J. F.; Balcells, D.; Sauer, E. L. O.; Raynaud, C.; Brudvig, G. W.; Crabtree, R. H.; Eisenstein, O. *J. Am. Chem. Soc.* **2010**, *132*, 7605–7616. (c) Cooper, H. L. R.; Mishra, G.; Huang, X.; Pender-Cudlip, M.; Austin, R. N.; Shanklin, J.; Groves, J. T. *J. Am. Chem. Soc.* **2012**, *134*, 20365–20375. (d) Usharani, D.; Janardanan, D.; Shaik, S. J. *Am. Chem. Soc.* **2011**, *133*, 176–179.
- (73) (a) Manka, M. J.; Stein, S. E. *J. Phys. Chem.* **1984**, *88*, 5914–5919. (b) Gibian, M. J.; Corley, R. C. *J. Am. Chem. Soc.* **1972**, *94*, 4178–4183.
- (74) (a) Çelenligil-Çetin, R.; Paraskevopoulou, P.; Dinda, R.; Lalioti, N.; Sanakis, Y.; Rawashdeh, A. M.; Staples, R. J.; Sinn, E.; Stavropoulos, P. *Eur. J. Inorg. Chem.* **2008**, 673–677. (b) Çelenligil-Çetin, R.; Paraskevopoulou, P.; Lalioti, N.; Sanakis, Y.; Staples, R. J.; Rath, N. P.; Stavropoulos, P. *Inorg. Chem.* **2008**, *47*, 10998–11009.